NFV Orchestration in Edge and Fog Scenarios

26th October, 2021

student: J. Martín-Pérez
supervisor: C. J. Bernardos

contact: jmartinp@it.uc3m.es

Motivation

To assess NFV orchestration in Edge & Fog:

To assess NFV orchestration in Edge & Fog:

1. graphs to represent 5G infrastructure

To assess NFV orchestration in Edge & Fog:

1. graphs to represent 5G infrastructure
2. service @local or @federated infrastructure

To assess NFV orchestration in Edge & Fog:

1. graphs to represent 5G infrastructure
2. service @local or @federated infrastructure
3. embed service in the infrastructure

To assess NFV orchestration in Edge & Fog:

1. graphs to represent 5G infrastructure
2. service @local or @federated infrastructure
3. embed service in the infrastructure
4. scale the embedded service

To assess NFV orchestration in Edge & Fog[1]:

1. graphs to represent 5G infrastructure
2. service @local or @federated infrastructure
3. embed service in the infrastructure
4. scale the embedded service

[1] The presentation focuses on the main thesis contributions.

Outline

uc3m

Outline

uc3m

uc3m

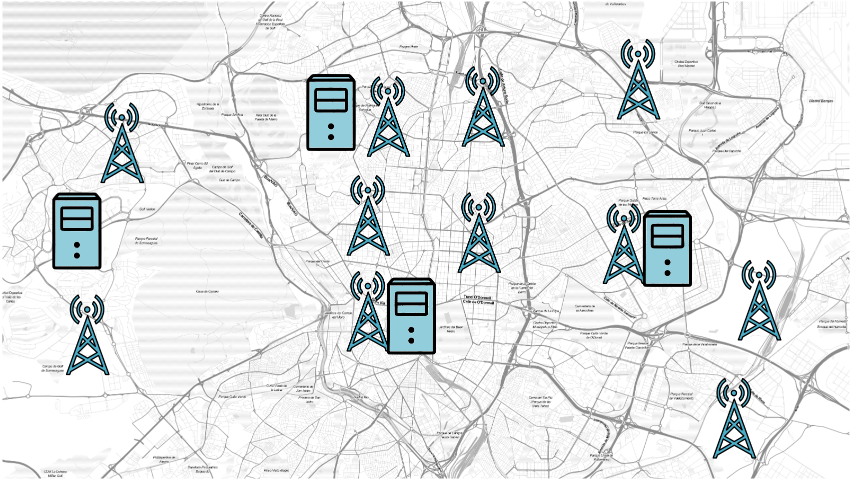

Figure 1: Illustration of BS and PoPs in Madrid

Location of BSs:

- Neyman-Scott Poisson Cluster Process [27]
- Poisson Point Processes (PPPs) [4]
  - homogeneous [28, 1]
  - hard-core [9]

Location of BSs:

- Neyman-Scott Poisson Cluster Process [27]
- Poisson Point Processes (PPPs) [4]
  - homogeneous [28, 1]
  - hard-core [9]
  - **inhomogeneous & Matérn II**

Location of BSs:

- Neyman-Scott Poisson Cluster Process [27]
- Poisson Point Processes (PPPs) [4]
  - homogeneous [28, 1]
  - hard-core [9]
  - **inhomogeneous & Matérn II**

Location of MEC PoPs:

- along highways [29]
- within stadiums [8]

Location of BSs:

- Neyman-Scott Poisson Cluster Process [27]
- Poisson Point Processes (PPPs) [4]
  - homogeneous [28, 1]
  - hard-core [9]
  - **inhomogeneous & Matérn II**

Location of MEC PoPs:

- along highways [29]
- within stadiums [8]
- population census
- access & aggregation rings

Derive:

- BS location
- MEC PoP location

Meet:

- Tactile RTT of **1 ms**

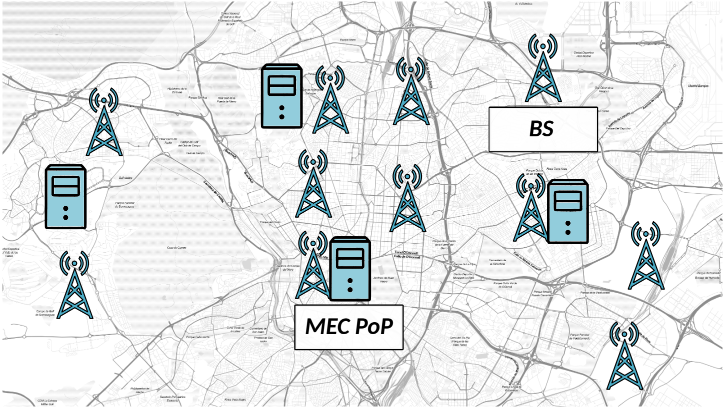

Figure 2: BS and MEC PoP locations

Higher gentrification $\implies$ more BSs

- R – region of interest
- C_i – area

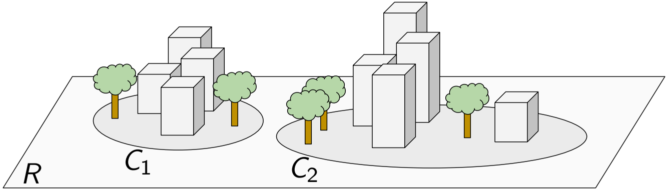

Figure 3: *Revolution functions* of a region with two building areas.

Higher gentrification $\implies$ more BSs

- R – region of interest
- C_i – area
- $f_i(x)$ – revolution func.

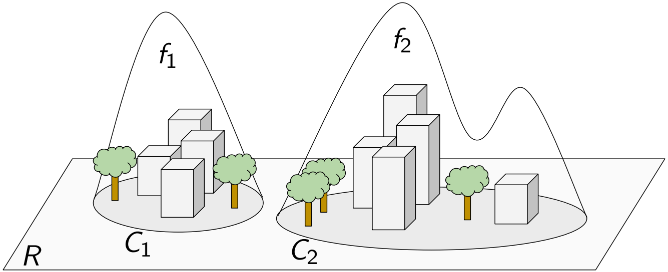

Figure 3: *Revolution functions* of a region with two building areas.

Higher gentrification $\implies$ more BSs

- R – region of interest
- C_i – area
- $f_i(x)$ – revolution func.
- $G(x)$ – gentrification
  - $G(x) = \sum_i f_i(x)$

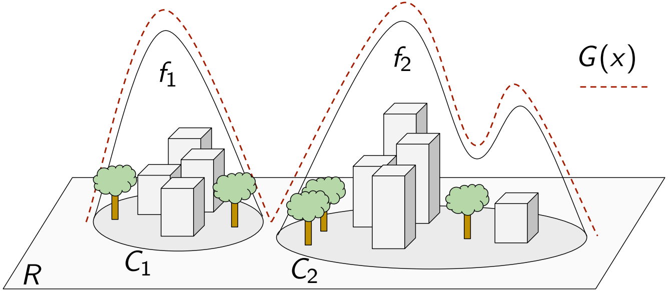

Figure 3: *Revolution functions* of a region with two building areas.

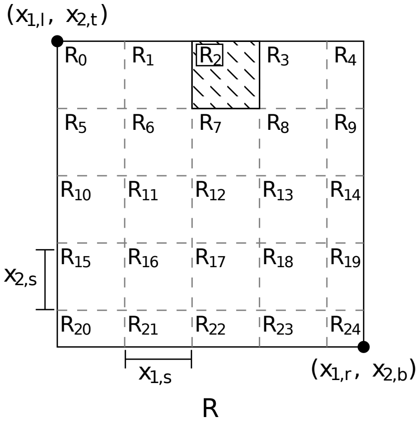

Figure 4: Gridded region

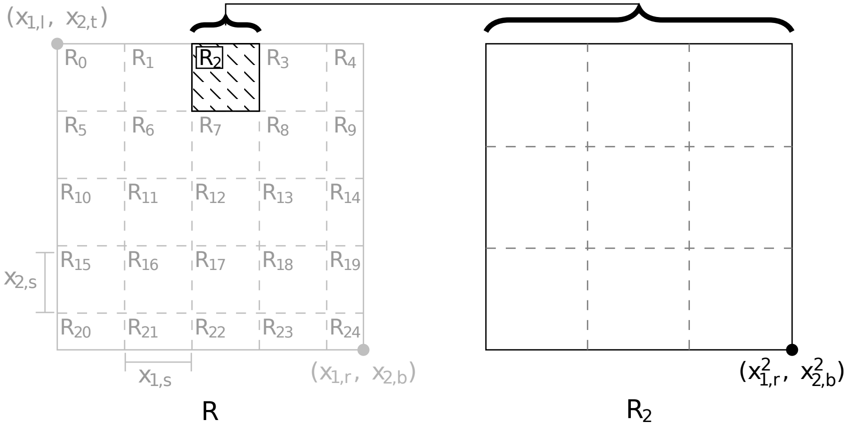

Figure 4: Gridded region (left), and inhomogeneous Mattérn II process of BSs (right).

BS intensity function $\lambda(x) \sim G(x)$ proportional to gentrification.

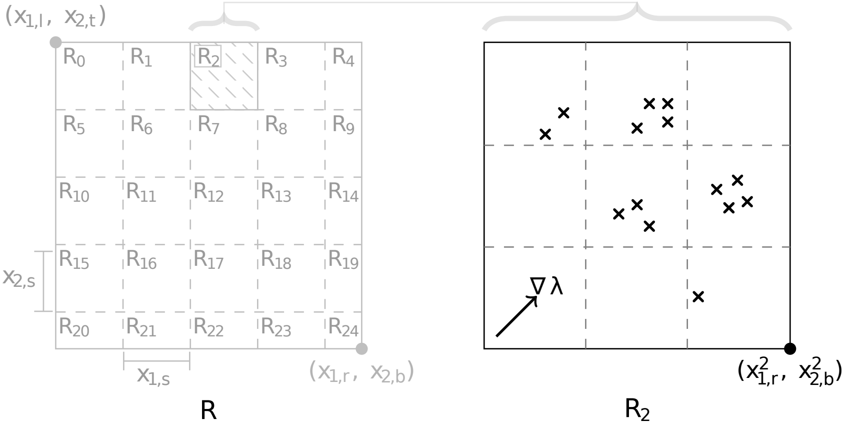

Figure 4: Gridded region (left), and inhomogeneous Mattérn II process of BSs (right).

BS intensity function $\lambda(x) \sim G(x)$ proportional to gentrification.

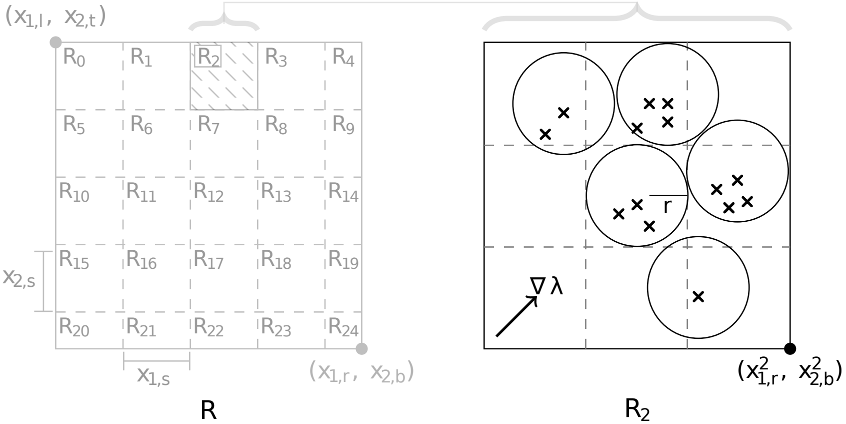

Figure 4: Gridded region (left), and inhomogeneous Mattérn II process of BSs (right).

BS intensity function $\lambda(x) \sim G(x)$ proportional to gentrification.

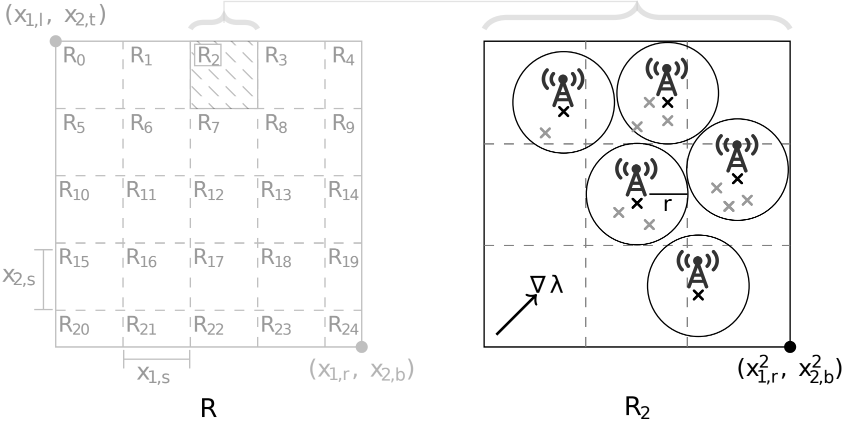

Figure 4: Gridded region (left), and inhomogeneous Mattérn II process of BSs (right).

uc3m

Inhomogeneous Mattérn II PPs applied on:

- R: Madrid city
- $G(x)$: Madrid census

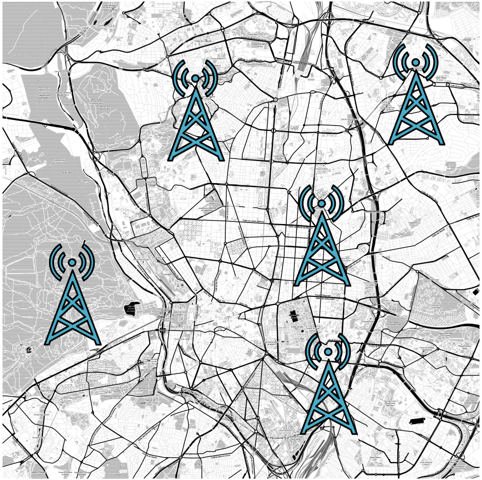

Figure 5: Location of BSs

uc3m

Inhomogeneous Mattérn II PPs applied on:

- R: Madrid city
- $G(x)$: Madrid census

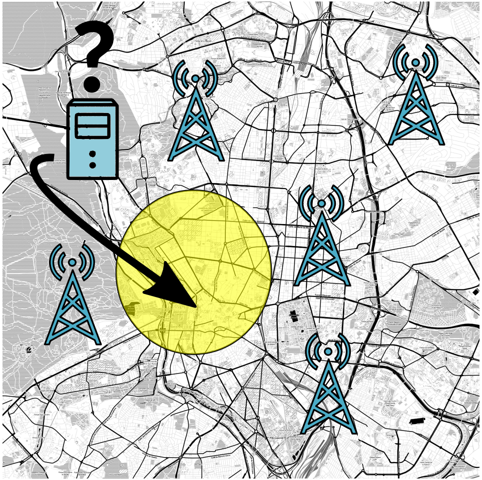

Figure 5: Location of BSs

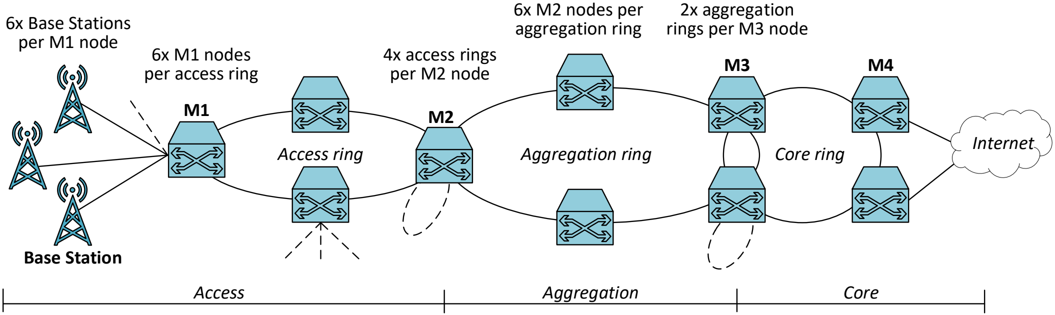

Figure 6: Reference network infrastructure as illustrated[2] in [6] and based on [10].

[2] Author: Dr. Luca Cominardi.

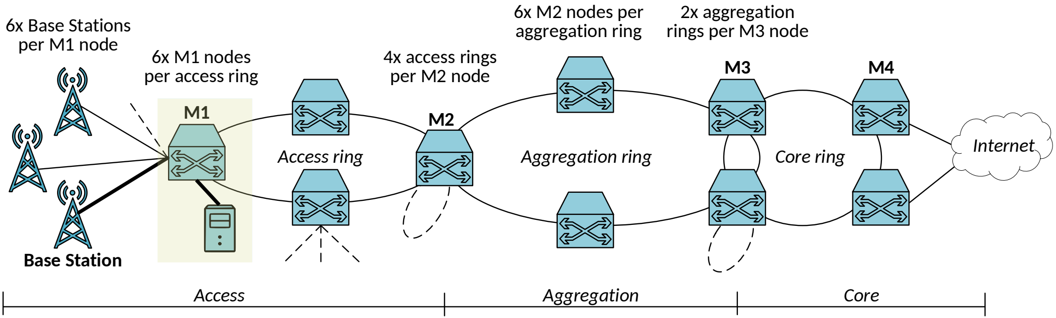

Figure 6: Reference network infrastructure as illustrated[2] in [6] and based on [10].

[2] Author: Dr. Luca Cominardi.

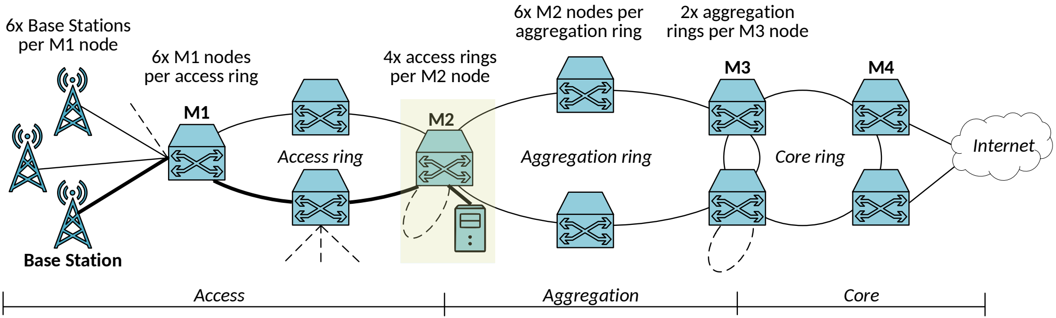

Figure 6: Reference network infrastructure as illustrated[2] in [6] and based on [10].

[2]Author: Dr. Luca Cominardi.

Derive MEC PoP location considering:

$$RTT = 2d \cdot 5\frac{\mu s}{km} + 2M \cdot 50\mu s + UL + DL \tag{1}$$

- d: distance between BS and MEC PoP
- M: #traversed rings (e.g., $1, 2, \ldots$)
- UL: Uplink propagation latency
- DL: Downlink propagation latency

Derive MEC PoP location considering:

$$RTT = \underbrace{2d \cdot 5\frac{\mu s}{km}}_{\text{fiber propagation}} + 2M \cdot 50\mu s + UL + DL \tag{1}$$

- d: distance between BS and MEC PoP
- M: #traversed rings (e.g., $1, 2, \ldots$)
- UL: Uplink propagation latency
- DL: Downlink propagation latency

Derive MEC PoP location considering:

$$RTT = 2d \cdot 5\frac{\mu s}{km} + \underbrace{2M \cdot 50\mu s}_{\text{ring propagation}} + UL + DL \tag{1}$$

- d: distance between BS and MEC PoP
- M: #traversed rings (e.g., $1, 2, \ldots$)
- UL: Uplink propagation latency
- DL: Downlink propagation latency

Derive MEC PoP location considering:

$$RTT = 2d \cdot 5\frac{\mu s}{km} + 2M \cdot 50\mu s + \underbrace{UL + DL}_{\text{radio propagation}} \quad (1)$$

- d: distance between BS and MEC PoP
- M: #traversed rings (e.g., $1, 2, \ldots$)
- UL: Uplink propagation latency
- DL: Downlink propagation latency

uc3m

m_M: maximum distance between MEC PoP at ring M and BS

Figure 7: How to select MEC PoP location

uc3m

m_2: maximum distance between MEC PoP at ring 2 and BS

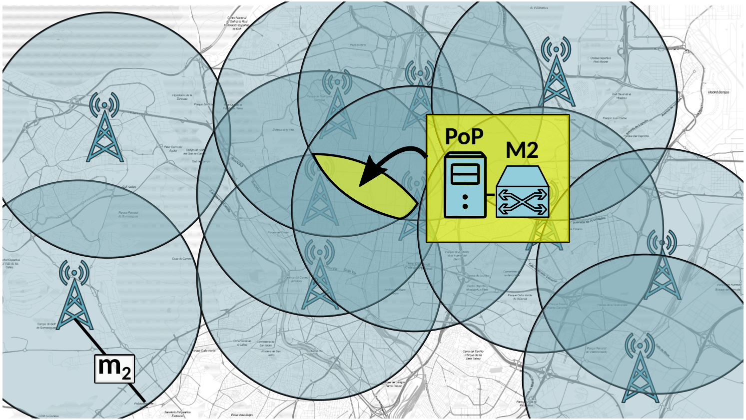

Figure 7: How to select MEC PoP location

uc3m

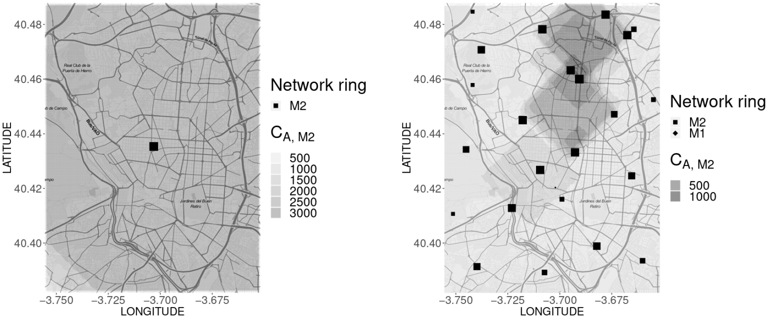

(a) FDD 120 kHz 7s (b) TDD 120 kHz 7s

Figure 8: **Urban scenario** (Madrid city center) – $C_{A,M2}$ =covered BSs

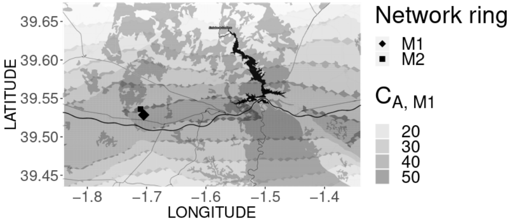

(a) FDD 120 kHz 7s

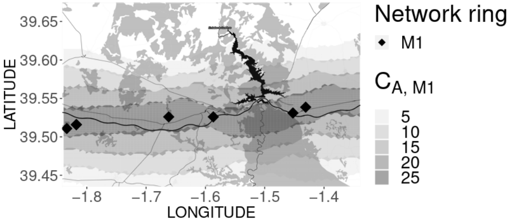

(b) TDD 120 kHz 7s

Figure 9: **Highway scenario** (Hoces del Cabriel A3) – $C_{A,M1}$ =covered BSs by M1 MEC PoP

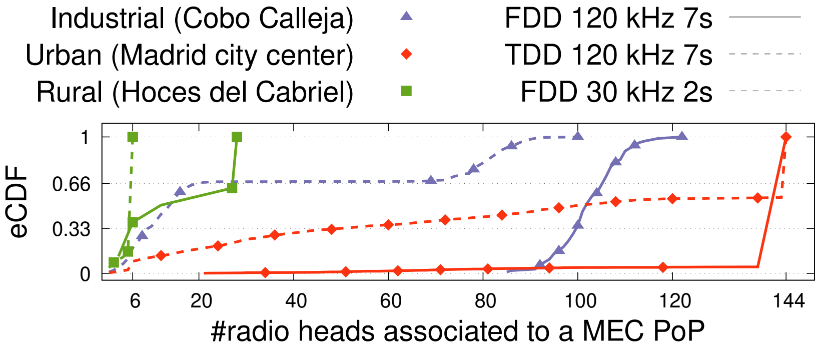

Figure 10: eCDF of the number of BSs assigned to a MEC PoP in the studied scenarios.

Publications:

- **Martín-Pérez, Jorge**, L. Cominardi, C. J. Bernardos, A. de la Oliva, and A. Azcorra. "Modeling Mobile Edge Computing Deployments for Low Latency Multimedia Services". In: *IEEE Transactions on Broadcasting* 65.2 (2019), pp. 464–474. DOI: 10.1109/TBC.2019.2901406
- **Martín-Pérez, Jorge**, L. Cominardi, C. J. Bernardos, and A. Mourad. "5GEN: A tool to generate 5G infrastructure graphs". In: *2019 IEEE Conference on Standards for Communications and Networking (CSCN)*. 2019, pp. 1–4. DOI: 10.1109/CSCN.2019.8931334

Open-source:

- **BS & MEC PoP generation**: `github.com/MartinPJorge/mec-generator/`
- **5GEN**: `https://github.com/MartinPJorge/mec-generator/tree/5g-infra-gen/`

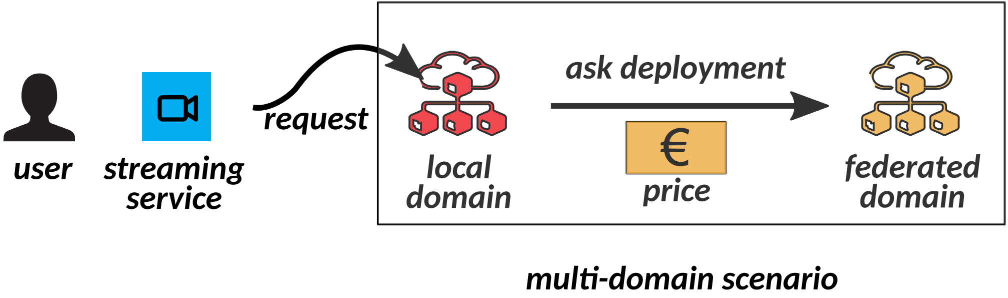

Figure 11: Service federation

Orchestration and **fixed pricing** in multi-domain:

- Alternating Direction Method of Multipliers (ADMM) [23]
- branching heuristic [11]
- graph-based message passing [33]
- greedy with backtracking [20]

Orchestration and **fixed pricing** in multi-domain:

- Alternating Direction Method of Multipliers (ADMM) [23]
- branching heuristic [11]
- graph-based message passing [33]
- greedy with backtracking [20]
- **cutoffs in Dijkstra, DFS and BFS [14]**
- **Q-learning federation [3]**

Orchestration and **fixed pricing** in multi-domain:

- Alternating Direction Method of Multipliers (ADMM) [23]
- branching heuristic [11]
- graph-based message passing [33]
- greedy with backtracking [20]
- **cutoffs in Dijkstra, DFS and BFS [14]**
- **Q-learning federation [3]**

Orchestration and **dynamic pricing** in multi-domain:

Orchestration and **fixed pricing** in multi-domain:

- Alternating Direction Method of Multipliers (ADMM) [23]
- branching heuristic [11]
- graph-based message passing [33]
- greedy with backtracking [20]
- **cutoffs in Dijkstra, DFS and BFS [14]**
- **Q-learning federation [3]**

Orchestration and **dynamic pricing** in multi-domain:

- **real-price traces AWS**

Orchestration and **fixed pricing** in multi-domain:

- Alternating Direction Method of Multipliers (ADMM) [23]
- branching heuristic [11]
- graph-based message passing [33]
- greedy with backtracking [20]
- **cutoffs in Dijkstra, DFS and BFS [14]**
- **Q-learning federation [3]**

Orchestration and **dynamic pricing** in multi-domain:

- **real-price traces AWS**
- **Deep Q-learning**

Orchestration and **fixed pricing** in multi-domain:

- Alternating Direction Method of Multipliers (ADMM) [23]
- branching heuristic [11]
- graph-based message passing [33]
- greedy with backtracking [20]
- **cutoffs in Dijkstra, DFS and BFS [14]**
- **Q-learning federation [3]**

Orchestration and **dynamic pricing** in multi-domain:

- **real-price traces AWS**
- **Deep Q-learning**
- **Telefónica scenario**

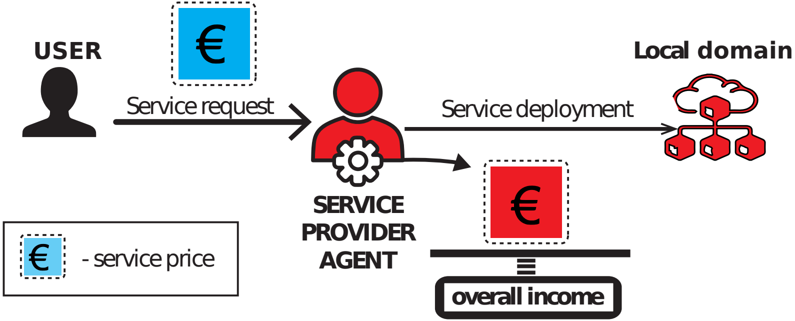

Figure 12: Business model - local deployment[3].

[3] Based on Kiril Antevski illustration

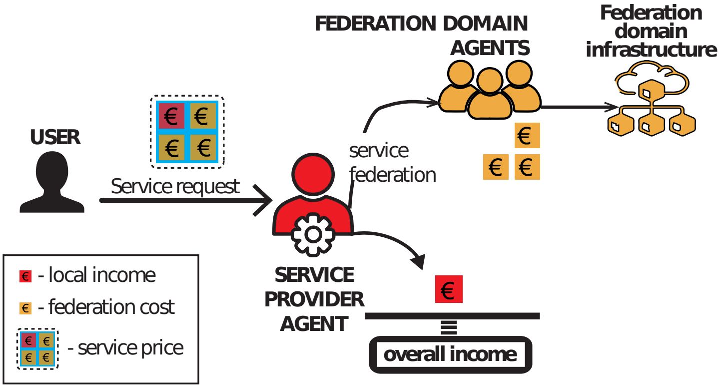

Figure 13: Business model - federate deployment[4].

[4] Based on Kiril Antevski illustration

t3a.small:

- 2 CPUs
- memory 2 GB
- storage 100 GB

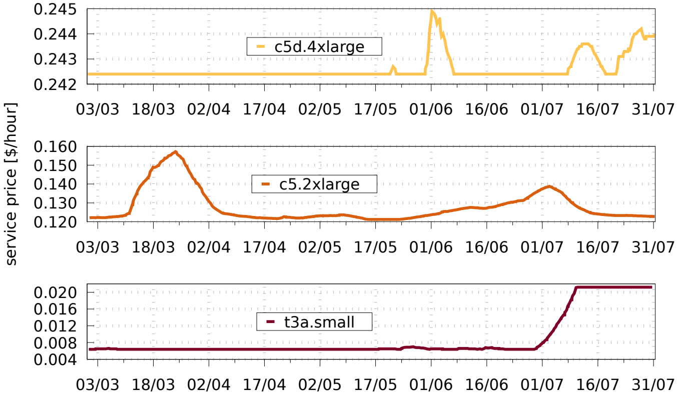

Figure 14: AWS service prices during 2020 in west Europe.

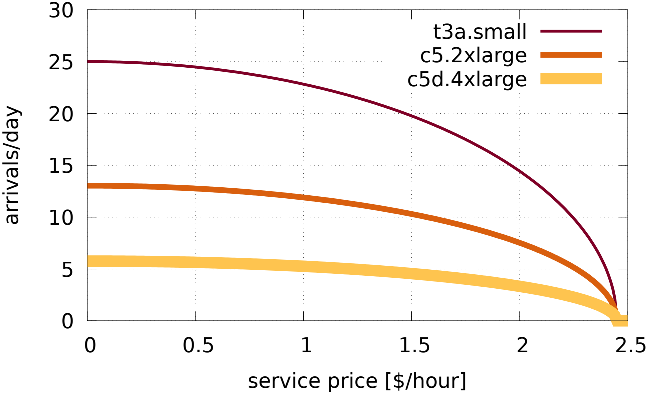

Figure 15: Impact of prices on arriving users – based on tid study [26] and [31].

Considering:

- Price changes
- Available resources (CPU, memory, disk)
- Service lifetime (e.g., 2 days)

Considering:

- Price changes
- Available resources (CPU, memory, disk)
- Service lifetime (e.g., 2 days)

For each service σ, decide / take an **action**:

- $x(\sigma) = 0$: **reject**
- $x(\sigma) = 1$: **local**
- $x(\sigma) = 2$: **federate**

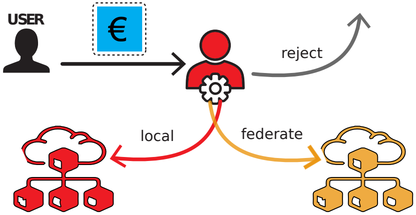

Figure 16: Possible actions.

uc3m

Obtained **reward**:

$$r^{(t)}(X_t) := \sum_{\substack{\sigma:\ x(\sigma)=0\\ a(\sigma)\leq t\leq d(\sigma)}} p^{a(\sigma)}(\sigma) + \sum_{\substack{\sigma:\ x(\sigma)=1\\ a(\sigma)\leq t\leq d(\sigma)}} \left[p^{a(\sigma)}(\sigma) - f^{(t)}(\sigma)\right] \quad (2)$$

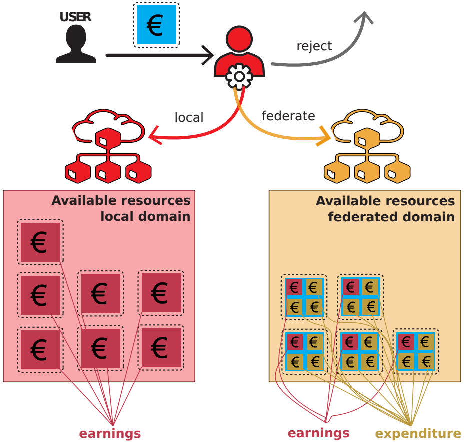

Figure 17: Environment snapshot at time t.

Obtained **reward**:

$$r^{(t)}(X_t) := \underbrace{\sum_{\substack{\sigma:\ x(\sigma)=0\\ a(\sigma)\leq t\leq d(\sigma)}} p^{a(\sigma)}(\sigma)}_{\text{local}} + \sum_{\substack{\sigma:\ x(\sigma)=1\\ a(\sigma)\leq t\leq d(\sigma)}} \left[p^{a(\sigma)}(\sigma) - f^{(t)}(\sigma)\right] \quad (2)$$

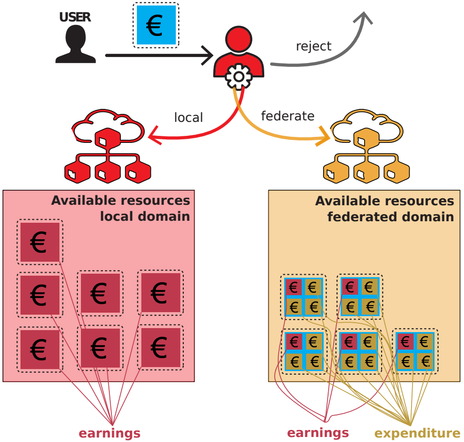

Figure 17: Environment snapshot at time t.

Obtained **reward**:

$$r^{(t)}(X_t) := \sum_{\substack{\sigma:\ x(\sigma)=0\\ a(\sigma)\leq t\leq d(\sigma)}} p^{a(\sigma)}(\sigma) + \sum_{\substack{\sigma:\ x(\sigma)=1\\ a(\sigma)\leq t\leq d(\sigma)}} \left[p^{a(\sigma)}(\sigma) - f^{(t)}(\sigma)\right] \quad (2)$$

federation

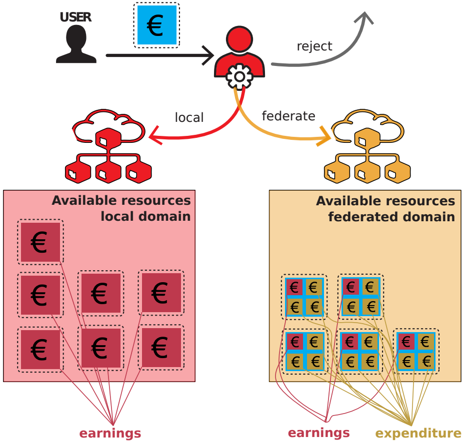

Figure 17: Environment snapshot at time t.

Online optimization problem:

- objective: $\max_{X_t} \frac{1}{T} \sum_t r^{(t)}(X_t)$
- constraints:
  - CPU
  - memory
  - disk

NP-hard: knapsack problem equivalence

Online optimization problem:

- objective: $\max_{X_t} \frac{1}{T} \sum_t r^{(t)}(X_t)$
- constraints:
  - CPU
  - memory
  - disk

NP-hard: knapsack problem equivalence

Markov Decision Problem (MDP):

- find policy π to:
  $\max_\pi \mathbb{E}_{x(\sigma)\sim\pi} \left[\sum_t \gamma^t \; r^{(t)}(\pi)\right]$
- action space $\mathcal{A} = \{0, 1, 2\}$
- state space $\mathcal{S}$:
  - available & requested resources
  - current prices
  - service lifetime
- instant reward $r^{(t)}(\pi)$

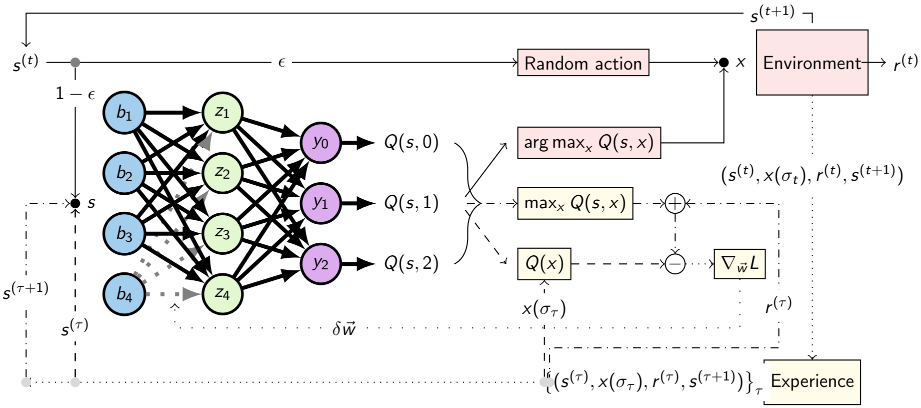

Figure 18: DQN architecture to decide rejection/local/federate.

Experimentation:

- Telefónica infrastructure & resources [26]

Experimentation:

- Telefónica infrastructure & resources [26]
- AWS prices dataset:
    - training 29/02/2020 – 02/05/2020
    - testing 03/05/2020 –31/07/2020

Experimentation:

- Telefónica infrastructure & resources [26]
- AWS prices dataset:
  - training 29/02/2020 – 02/05/2020
  - testing 03/05/2020 –31/07/2020
- Poissonian arrival of users

Comparison of:

- Optimal
- DQN
- Q-table
- Q-table explore
- greedy

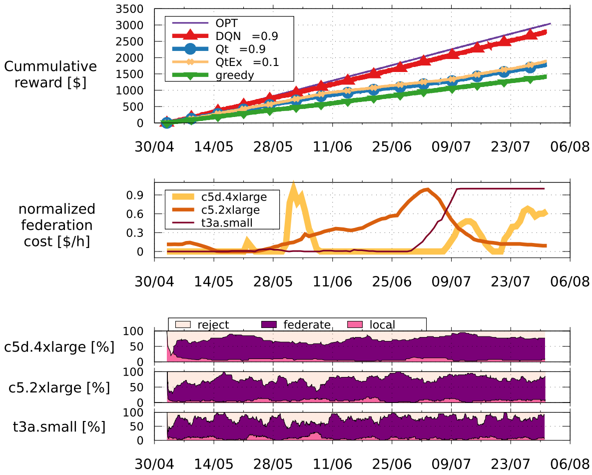

Figure 19: federation agents' performance.

Comparison of:

- Optimal
- DQN
- Q-table
- Q-table explore
- greedy

Results:

- near-optimal

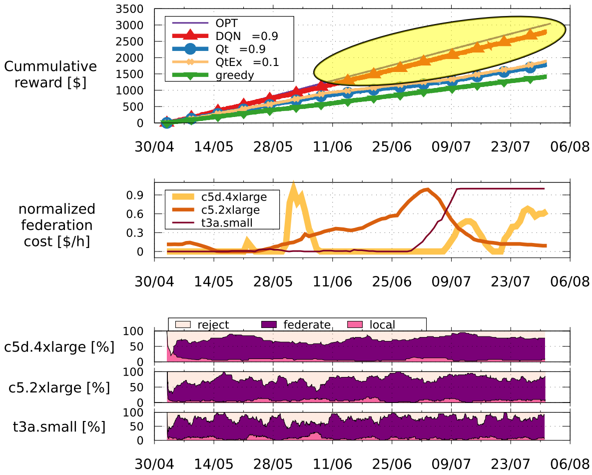

Figure 19: federation agents' performance.

uc3m

Comparison of:

- Optimal
- DQN
- Q-table
- Q-table explore
- greedy

Results:

- near-optimal
- react upon peaks

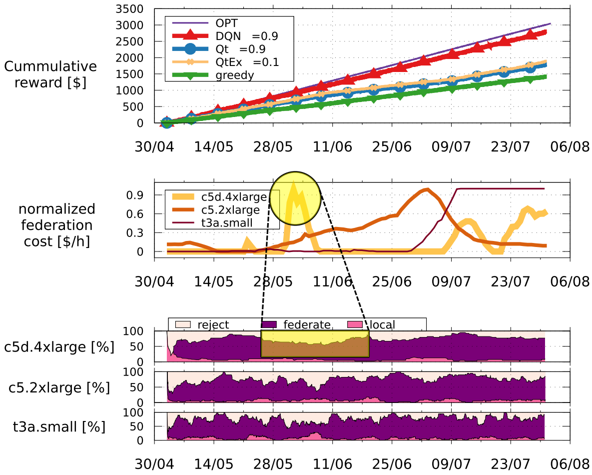

Figure 19: federation agents' performance.

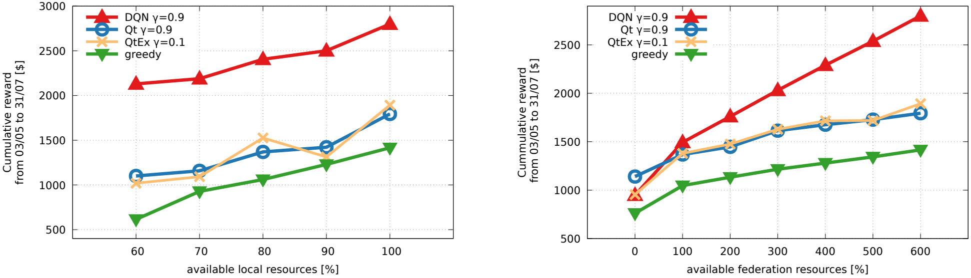

(a) Increasing local resources.

(b) Increasing resources in federation.

Figure 20: Cumulative reward vs. available resources

Publications:

- **Martín-Pérez, Jorge** and C. J. Bernardos. "Multi-Domain VNF Mapping Algorithms". In: *2018 IEEE International Symposium on Broadband Multimedia Systems and Broadcasting (BMSB)*. 2018, pp. 1–6. DOI: 10.1109/BMSB.2018.8436765
- K. Antevski, **J. Martín-Pérez**, A. Garcia-Saavedra, C. J. Bernardos, X. Li, J. Baranda, J. Mangues-Bafalluy, R. Martnez, and L. Vettori. "A Q-learning strategy for federation of 5G services". In: *ICC 2020 - 2020 IEEE International Conference on Communications (ICC)*. 2020, pp. 1–6. DOI: 10.1109/ICC40277.2020.9149082
- **Martín-Pérez, Jorge**, K. Antevski, A. Garcia-Saavedra, X. Li, and C. J. Bernardos. "DQN Dynamic Pricing and Revenue driven Service Federation Strategy". In: *IEEE Transactions on Network and Service Management* (2021), pp. 1–1. DOI: 10.1109/TNSM.2021.3117589

Open-source:

- **DFS, BFS w/ cutoffs**: `https://github.com/MartinPJorge/placement/`
- **Q-table**: `https://github.com/MartinPJorge/5gt-federation/`
- **DQN & environment**: `https://github.com/MartinPJorge/5gt-federation/tree/extensionICC/utils/aws/`

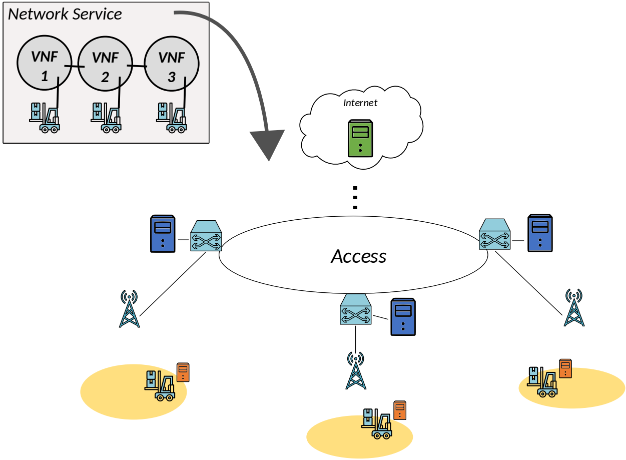

Figure 21: Virtual Network Function Embedding (VNE).

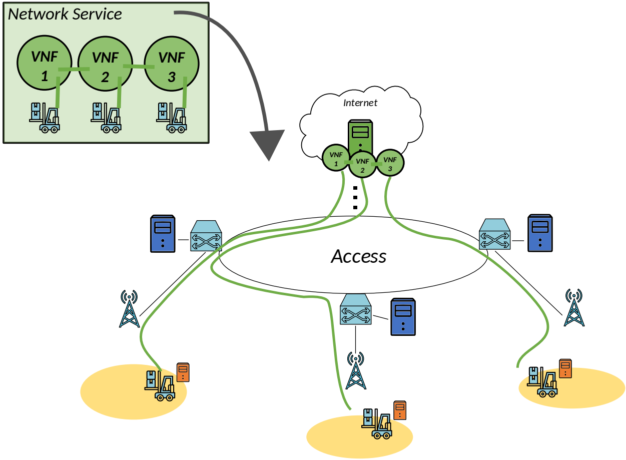

Figure 21: Virtual Network Function Embedding (VNE).

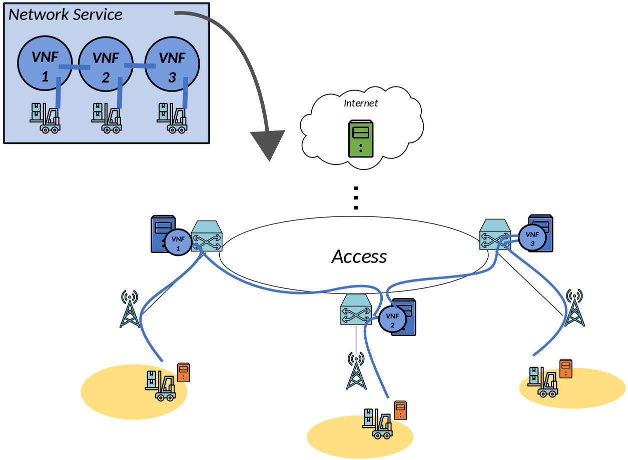

Figure 21: Virtual Network Function Embedding (VNE).

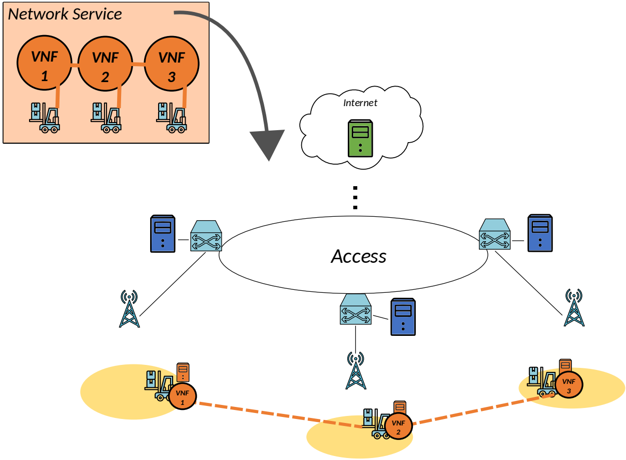

Figure 21: Virtual Network Function Embedding (VNE).

Existing Virtual Network Embedding (VNE) solutions:

- latency-aware, bipartite graph & Hungarian [12]
- maxZ: latency-aware, relaxed ILP [2]
- z-TORCH: KPI monitoring, k-means VNF assign [25]
- AIA: meet latency and throughput [32]

Existing Virtual Network Embedding (VNE) solutions:

- latency-aware, bipartite graph & Hungarian [12]
- maxZ: latency-aware, relaxed ILP [2]
- z-TORCH: KPI monitoring, k-means VNF assign [25]
- AIA: meet latency and throughput [32]

OKpi accounts for:

- latency constraints
- **radio coverage**
- **geographical availability**
- **reliability**

Latency constraint $D(s)$:

$$d_{\text{net}}(\psi) + d_{\text{proc}} \leq D(s) \qquad (3)$$

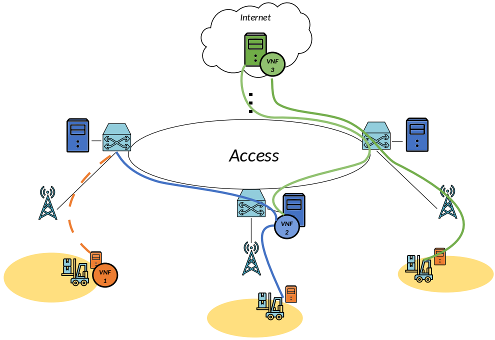

Figure 22: Service s delay.

Latency constraint $D(s)$:

$$\underbrace{d_{\text{net}}(\psi)}_{\text{propagation delay}} + d_{\text{proc}} \leq D(s) \quad (3)$$

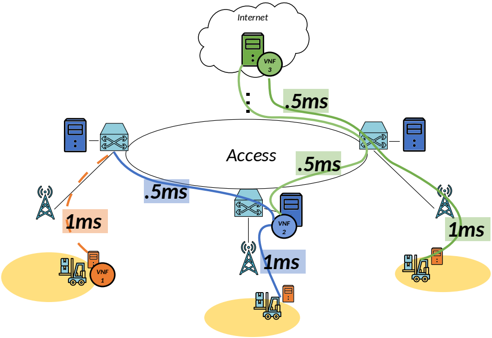

Figure 22: Service s delay.

Latency constraint $D(s)$:

$$d_{\text{net}}(\psi) + \underbrace{d_{\text{proc}}(\psi)}_{\text{processing delay}} \leq D(s) \quad (3)$$

d_{proc}: VNF as M/M/1-PS queue

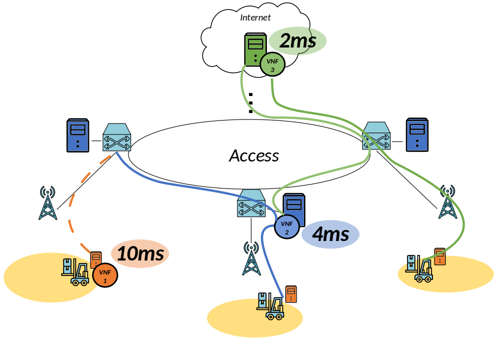

Figure 22: Service s delay.

Radio technology *i* constraint:

$$\rho(v,c)r_i(v) \leq R_i(c) \qquad (4)$$

- $\rho(v,c)$: VNF v is deployed in c
- $R_i(c)$: radio point of access c has radio technology i
- $r_i(v)$: VNF v needs radio technology i

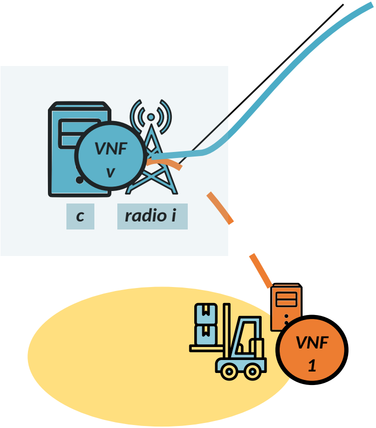

Figure 23: Radio VNF.

Geographical availability:

$$\forall \psi = (\alpha, s), \exists c, v_1, v_2 : \quad \tau_{\psi,c}(e, v_1, v_2) > 0 \quad (5)$$

- location α
- $\tau_{e,c}(e, v_1, v_2)$: flow (ψ, v_1, v_2) traverses link (ψ, c)

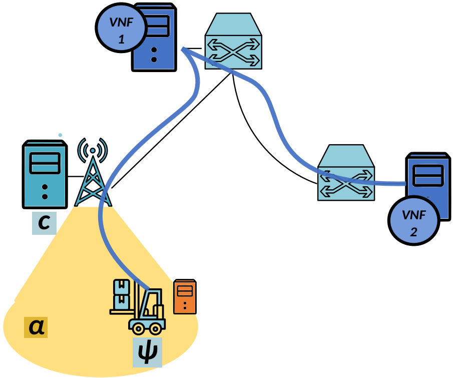

Figure 24: coverage of region α.

Service **reliability** $H(s)$:

$$\prod_{\substack{v_1, v_2 \in \mathcal{V} \\ (i,j) \in w}} \eta(j,t)\eta(i,j,t) \geq H(s) \quad (6)$$

- $\eta(j,t)$: node reliability at t
- $\eta(i,j,t)$: node reliability at t

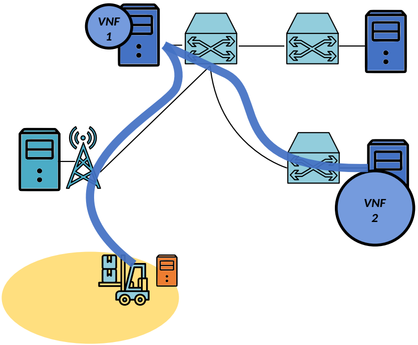

Figure 25: Traffic path.

Service **reliability** $H(s)$:

$$\prod_{v_1,v_2\in\mathcal{V}} \sum_{w\in\mathcal{W}} \underbrace{f(\psi, v_1, v_2, w)}_{\text{traffic fraction}} \prod_{(i,j)\in w} \eta(j,t)\eta(i,j,t) \geq H(s) \quad (6)$$

- $\eta(j,t)$: node reliability at t
- $\eta(i,j,t)$: node reliability at t
- w: traffic path

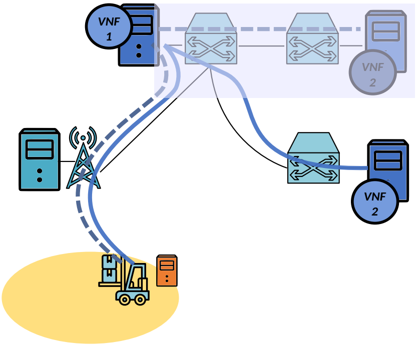

Figure 25: Fractioned traffic path.

Formulate an optimization problem:

$$\min \sum_{c} \sum_{v} \left[c_c(v) + \sum_{e} \sum_{\kappa} c_c(\kappa) a_c(\psi, v, \kappa) \right] + \sum_{(i,j)} \sum_{e} \sum_{v_1, v_2} c_{i,j} \tau_{i,j}(\psi, v_1, v_2) \tag{7}$$

$$s.t. (3) - (6) \tag{8}$$

Formulate an optimization problem:

$$\min \sum_{c} \sum_{v} \left[\underbrace{c_c(v)}_{\text{VNF cost}} + \sum_{e} \sum_{\kappa} c_c(\kappa) a_c(\psi, v, \kappa) \right] + \sum_{(i,j)} \sum_{e} \sum_{v_1, v_2} c_{i,j} \tau_{i,j}(\psi, v_1, v_2) \quad (7)$$

$$s.t. (3) - (6) \quad (8)$$

Formulate an optimization problem:

$$\min \sum_{c} \sum_{v} \left[c_c(v) + \sum_{e} \sum_{\kappa} \underbrace{c_c(\kappa) a_c(\psi, v, \kappa)}_{\text{assigned resource } \kappa \text{ cost}} \right] + \sum_{(i,j)} \sum_{e} \sum_{v_1, v_2} c_{i,j} \tau_{i,j}(\psi, v_1, v_2) \tag{7}$$

$$s.t. (3) - (6) \tag{8}$$

Formulate an optimization problem:

$$\min \sum_{c} \sum_{v} \left[c_c(v) + \sum_{e} \sum_{\kappa} c_c(\kappa) a_c(\psi, v, \kappa) \right] + \sum_{(i,j)} \sum_{e} \sum_{v_1, v_2} \underbrace{c_{i,j} \tau_{i,j}(\psi, v_1, v_2)}_{\text{traffic steering cost}} \tag{7}$$

$$s.t. (3) - (6) \tag{8}$$

Formulate an optimization problem:

$$\min \sum_{c} \sum_{v} \left[c_c(v) + \sum_{e} \sum_{\kappa} c_c(\kappa) a_c(\psi, v, \kappa) \right] + \sum_{(i,j)} \sum_{e} \sum_{v_1, v_2} c_{i,j} \tau_{i,j}(\psi, v_1, v_2) \tag{7}$$

$$s.t. (3) - (6) \tag{8}$$

NP-hard: bin-packing problem equivalence.

The **OKpi** (all KPI) solution:

- infrastructure as a graph
- edges with:
  - delay
  - reliability

The **OKpi** (all KPI) solution:

- infrastructure as a graph
- edges with:
  - delay
  - reliability

Solve in two steps:

1. Create a decision graph
2. Create an expanded graph

Decision graph $\tilde{G} = (\tilde{N}, \tilde{E})$.

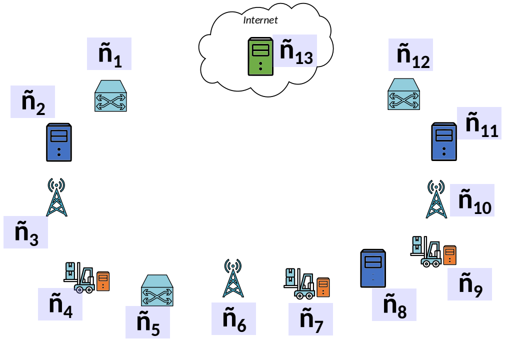

Figure 26: OKpi decision graph.

Decision graph $\tilde{G} = (\tilde{N}, \tilde{E})$.

Nodes $\tilde{N} = \{\tilde{n}_1, \tilde{n}_2, \ldots\}$:

- $|\mathcal{V}| - 1$ replicas

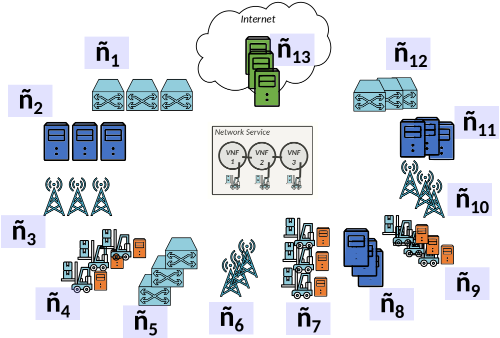

Figure 26: OKpi decision graph.

Decision graph $\tilde{G} = (\tilde{N}, \tilde{E})$.

Nodes $\tilde{N} = \{\tilde{n}_1, \tilde{n}_2, \dots\}$:

- $|\mathcal{V}| - 1$ replicas

Edges $\tilde{E} = \{(\tilde{n}_1, \tilde{n}_2), \dots\}$:

- two weights:

$$\left(\frac{\tilde{D}_{\tilde{n}_1,\tilde{n}_2}}{D(s)}, \frac{\log \tilde{\eta}_{\tilde{n}_1,\tilde{n}_2}}{\log H(s)} \right) \tag{9}$$

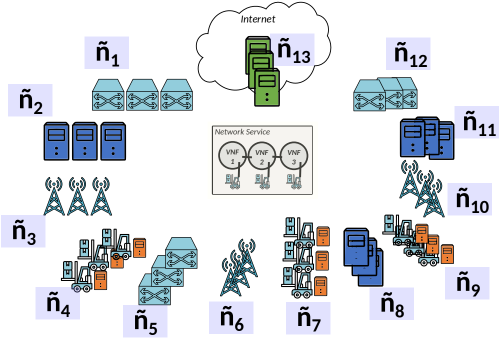

Figure 26: OKpi decision graph.

Decision graph $\tilde{G} = (\tilde{N}, \tilde{E})$.

Nodes $\tilde{N} = \{\tilde{n}_1, \tilde{n}_2, \dots\}$:

- $|\mathcal{V}| - 1$ replicas

Edges $\tilde{E} = \{(\tilde{n}_1, \tilde{n}_2), \dots\}$:

- two weights:

$$\left(\underbrace{\frac{\tilde{D}_{\tilde{n}_1,\tilde{n}_2}}{D(s)}}_{\text{delay fraction}}, \frac{\log \tilde{\eta}_{\tilde{n}_1,\tilde{n}_2}}{\log H(s)} \right) \tag{9}$$

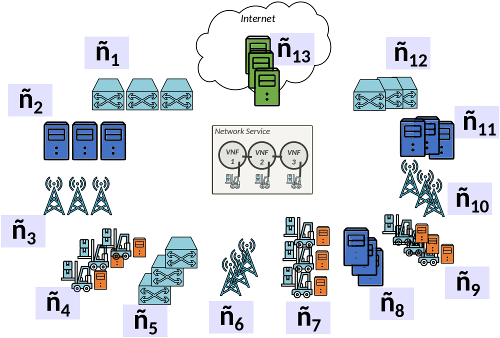

Figure 26: OKpi decision graph.

Decision graph $\tilde{G} = (\tilde{N}, \tilde{E})$.

Nodes $\tilde{N} = \{\tilde{n}_1, \tilde{n}_2, \ldots\}$:

- $|\mathcal{V}| - 1$ replicas

Edges $\tilde{E} = \{(\tilde{n}_1, \tilde{n}_2), \ldots\}$:

- two weights:

$$\left(\frac{\tilde{D}_{\tilde{n}_1,\tilde{n}_2}}{D(s)}, \underbrace{\frac{\log \tilde{\eta}_{\tilde{n}_1,\tilde{n}_2}}{\log H(s)}}_{\text{reliability fraction}} \right) \tag{9}$$

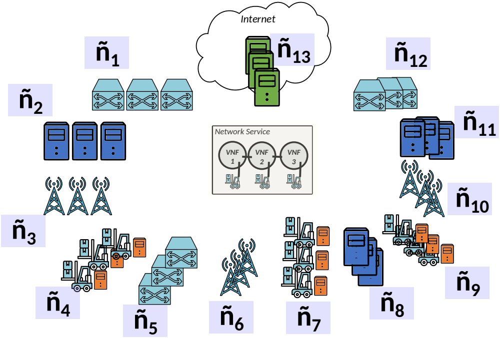

Figure 26: OKpi decision graph.

Decision graph $\tilde{G} = (\tilde{N}, \tilde{E})$.

Nodes $\tilde{N} = \{\tilde{n}_1, \tilde{n}_2, \dots\}$:

- $|\mathcal{V}| - 1$ replicas

Edges $\tilde{E} = \{(\tilde{n}_1, \tilde{n}_2), \dots\}$:

- two weights:

$$\left(\frac{\tilde{D}_{\tilde{n}_1,\tilde{n}_2}}{D(s)}, \frac{\log \tilde{\eta}_{\tilde{n}_1,\tilde{n}_2}}{\log H(s)}\right) \quad (9)$$

- create links $(\tilde{n}_1, \tilde{n}_2)$

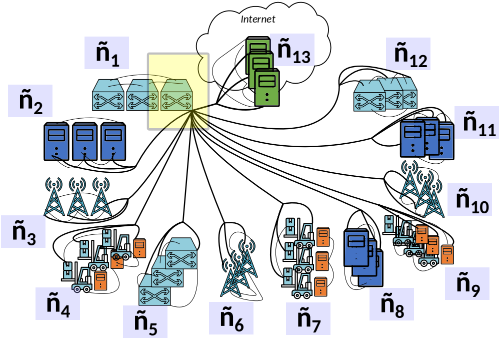

Figure 26: OKpi decision graph.

Expanded graph:

1. add superscripts $\tilde{n}^{d,r}$
   - d: delay to reach it
   - r: reliab. to reach it

Figure 27: OKpi expanded graph $\gamma = 3$.

Expanded graph:

1. add superscripts $\tilde{n}^{d,r}$
   - d: delay to reach it
   - r: reliab. to reach it
2. add $(\gamma+1)^2$ replicas

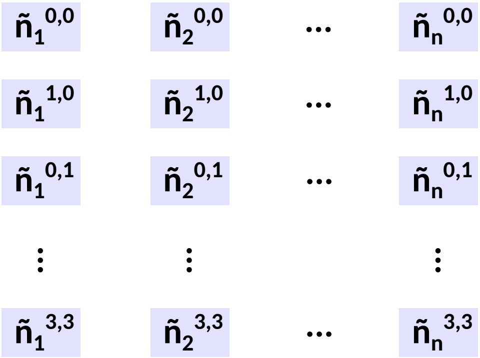

Figure 27: OKpi expanded graph $\gamma = 3$.

Expanded graph:

1. add superscripts $\tilde{n}^{d,r}$
   - d: delay to reach it
   - r: reliab. to reach it
2. add $(\gamma+1)^2$ replicas
3. connect $\tilde{n}_1{}^{d_1,r_2}$ with $\tilde{n}_2{}^{d_2,r_2}$

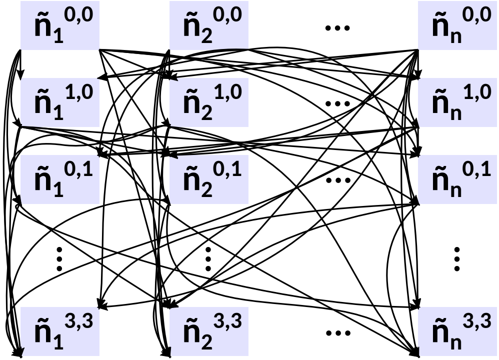

Figure 27: OKpi expanded graph $\gamma = 3$.

Expanded graph:

1. add superscripts $\tilde{n}^{d,r}$
   - d: delay to reach it
   - r: reliab. to reach it
2. add $(\gamma+1)^2$ replicas
3. connect $\tilde{n}_1{}^{d_1,r_2}$ with $\tilde{n}_2{}^{d_2,r_2}$
   - link $(\tilde{n}_1,\tilde{n}_2)\in\tilde{E}$
   - $d_1+\gamma\cdot d(\tilde{n}_1,\tilde{n}_2)\leq d_2$
   - $r_1+\gamma\cdot r(\tilde{n}_1,\tilde{n}_2)\leq r_2$

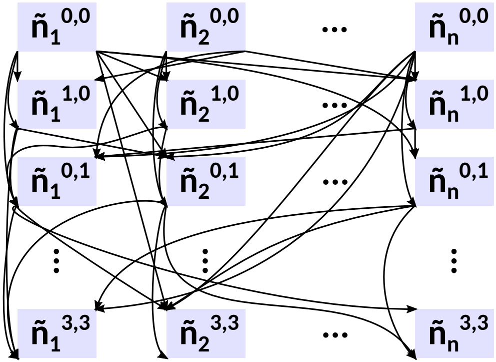

Figure 27: OKpi expanded graph $\gamma=3$.

uc3m

Expanded graph:

1. add superscripts $\tilde{n}^{d,r}$
   - d: delay to reach it
   - r: reliab. to reach it
2. add $(\gamma+1)^2$ replicas
3. connect $\tilde{n}_1{}^{d_1,r_2}$ with $\tilde{n}_2{}^{d_2,r_2}$
   - link $(\tilde{n}_1, \tilde{n}_2) \in \tilde{E}$
   - $d_1 + \gamma \cdot d(\tilde{n}_1, \tilde{n}_2) \leq d_2$
   - $r_1 + \gamma \cdot r(\tilde{n}_1, \tilde{n}_2) \leq r_2$
4. one hop per VNF

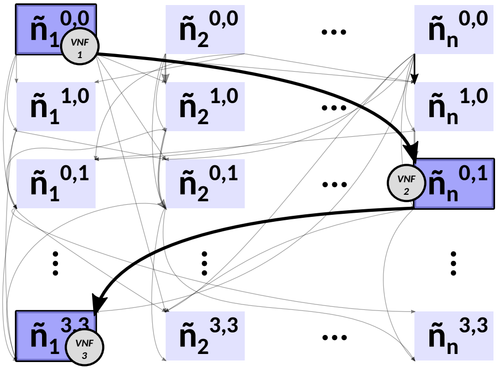

Figure 27: OKpi expanded graph $\gamma = 3$.

Expanded graph:

1. add superscripts $\tilde{n}^{d,r}$
   - d: delay to reach it
   - r: reliab. to reach it
2. add $(\gamma+1)^2$ replicas
3. connect $\tilde{n}_1{}^{d_1,r_2}$ with $\tilde{n}_2{}^{d_2,r_2}$
   - link $(\tilde{n}_1, \tilde{n}_2) \in \tilde{E}$
   - $d_1 + \gamma \cdot d(\tilde{n}_1, \tilde{n}_2) \leq d_2$
   - $r_1 + \gamma \cdot r(\tilde{n}_1, \tilde{n}_2) \leq r_2$
4. one hop per VNF

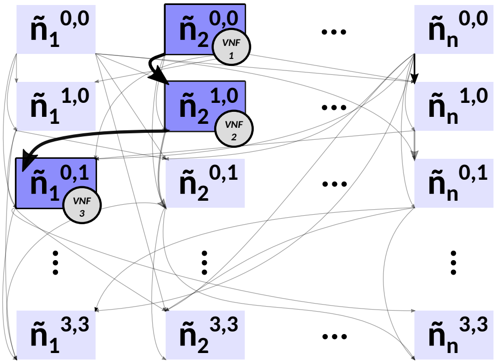

Figure 27: OKpi expanded graph $\gamma = 3$.

Simulations using realistic ITU+3GPP 5G scenarios [16]:

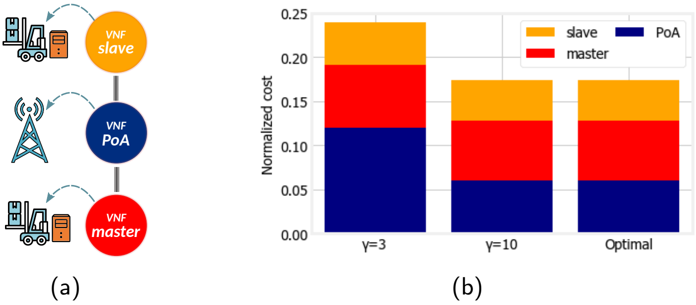

Figure 28: (a) master-slave robotic VS illustration, and (b) optimality comparison of the VNFs' deployment costs using OKpi with $\gamma = 3, 10$.

Simulations using realistic ITU+3GPP 5G scenarios [16]:

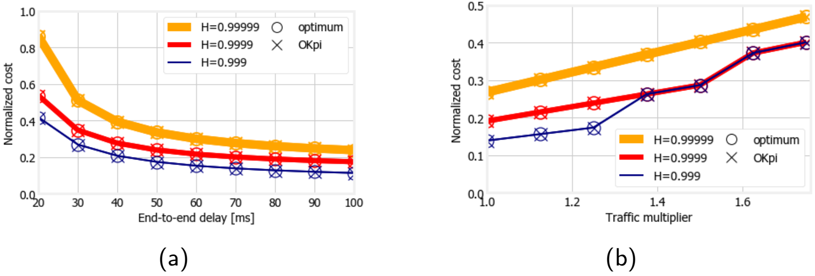

Figure 29: (a) end-to-end delay, and (b) traffic impact on deployment cost of master-slave robotic VS

Outline

uc3m

uc3m

Publications:

- **Martín-Peréz, Jorge**, F. Malandrino, C. F. Chiasserini, and C. J. Bernardos. "OKpi: All-KPI Network Slicing Through Efficient Resource Allocation". In: *IEEE INFOCOM 2020 - IEEE Conference on Computer Communications*. 2020, pp. 804–813. DOI: 10.1109/INFOCOM41043.2020.9155263
- **Martín-Peréz, Jorge**, F. Malandrino, C. F. Chiasserini, M. Groshev, and C. J. Bernardos. "KPI Guarantees in Network Slicing". In: *IEEE/ACM Transactions on Networking* (2021). Accepted
- B. Nemeth, N. Molner, **Martín-Pérez, J.**, C. J. Bernardos, A. de la Oliva, and B. Sonkoly. "Delay and reliability-constrained VNF placement on mobile and volatile 5G infrastructure". In: *IEEE Transactions on Mobile Computing* (2021), pp. 1–1. DOI: 10.1109/TMC.2021.3055426

Open-source:

- **AMPLPY**: `https://github.com/ampl/amplpy/`
- **networkx**: `https://github.com/networkx/networkx/`
- **OKpi**: `https://github.com/MartinPJorge/placement/`
- **FMC**: `https://github.com/MartinPJorge/placement/`

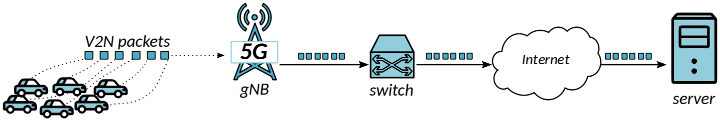

Figure 30: V2N service scaling.

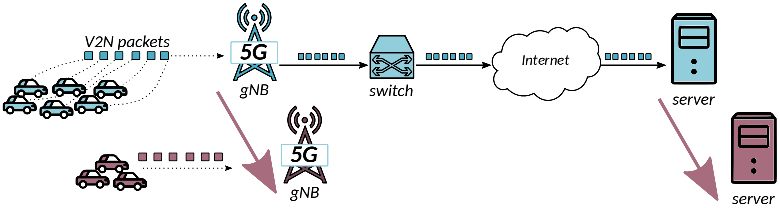

Figure 30: V2N service scaling.

V2N scaling solutions:

- asign radio resource blocks [22]
- computing resources scaling:
  - threshold-based [5, 24]
  - LSTM-based [7]

V2N scaling solutions:

- asign radio resource blocks [22]
- computing resources scaling:
  - threshold-based [5, 24]
  - LSTM-based [7]
  - **compare**:
    - DES, TES
    - HTM
    - GRU
    - LSTM
    - TCN
    - TCNLSTM

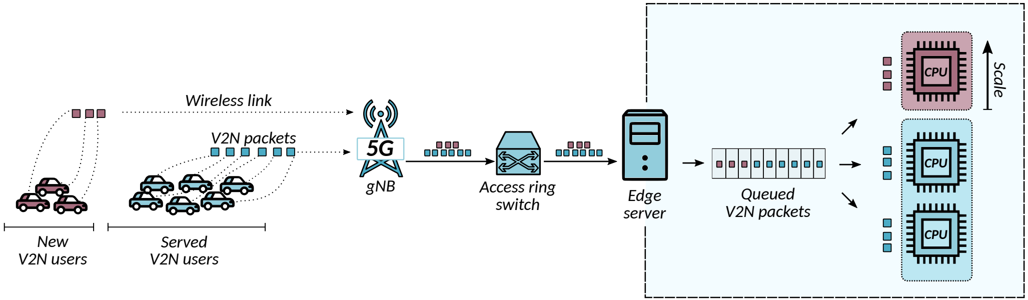

Figure 31: V2N service vertical scaling.

Edge server – $M/M/c$ queue:

- $\lambda(t)$: cars' arrival rate
- μ: CPU service rate
- $c(t)$: number of CPUs

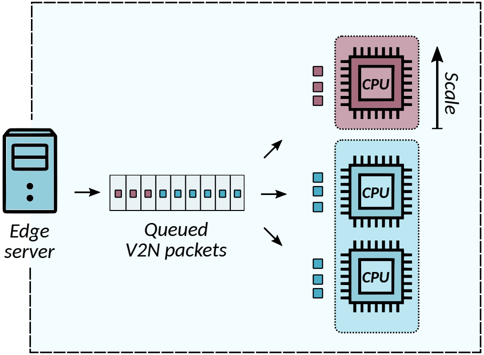

Figure 32: Server as $M/M/c$ queue.

Edge server – $M/M/c$ queue:

- $\lambda(t)$: cars' arrival rate
- μ: CPU service rate
- $c(t)$: number of CPUs

Scale to meet avg. latency:

$$\frac{1}{\mu} + \frac{P_Q}{c(t)\mu - \lambda(t)} \tag{10}$$

with P_Q the prob. of all servers bussy (Earlang C).

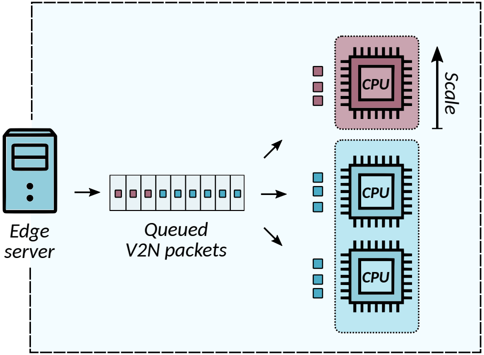

Figure 32: Server as $M/M/c$ queue.

Dataset to derive $\lambda(t)$:

- 116 roads in Torino
- (lat,lng) of roads
- traffic [vehicles/hour] each 5 min.
- avg. speed [vehicles/hour] each 5 min.
- from 28/01/2020 – now

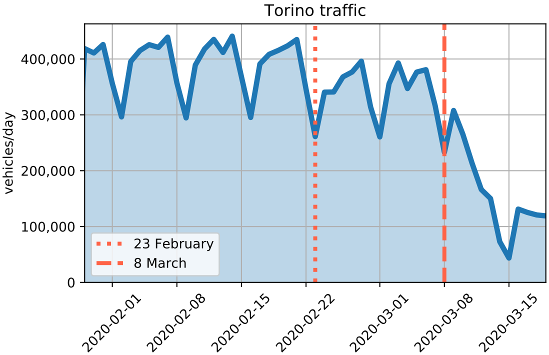

Figure 33: Traffic after COVID-19 lockdowns – 8 March.

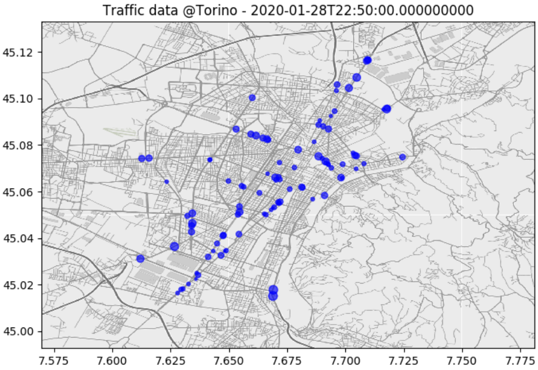

Figure 34: Vehicular traffic – wee hours @Torino.

Predict future traffic $\lambda(t+n)$

- **time-series techniques**: DES, TES
- **proprietary**: HTM
- **neural networks**: GRU, LSTM, TCN, TCNLSTM

Patterns:

- strong **seasonality**.

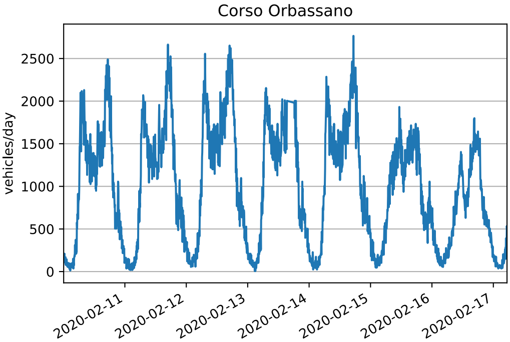

Figure 35: Weekly traffic at Corso Orbassano road.

Predict future traffic $\lambda(t+n)$

- **time-series techniques**: DES, TES
- **proprietary**: HTM
- **neural networks**: GRU, LSTM, TCN, TCNLSTM

Patterns:

- strong **seasonality**.
- week & weekend flows

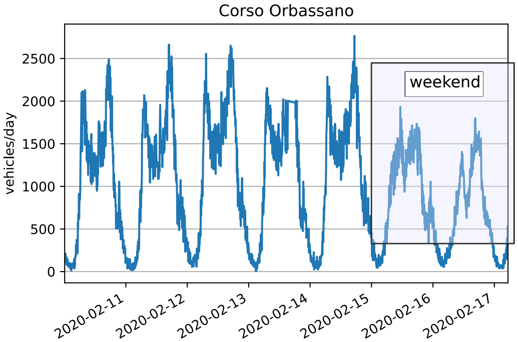

Figure 35: Weekly traffic at Corso Orbassano road.

Predict future traffic $\lambda(t + n)$

- **time-series techniques**: DES, TES
- **proprietary**: HTM
- **neural networks**: GRU, LSTM, TCN, TCNLSTM

Patterns:

- strong **seasonality**.
- week & weekend flows
- night hours,

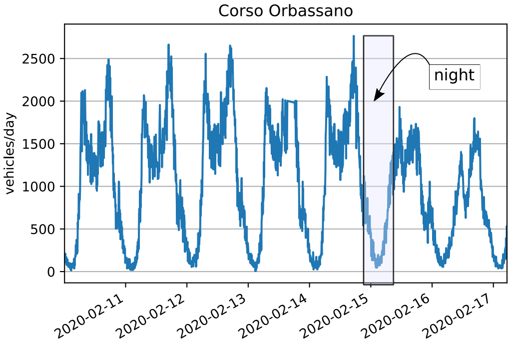

Figure 35: Weekly traffic at Corso Orbassano road.

Predict future traffic $\lambda(t+n)$

- **time-series techniques**: DES, TES
- **proprietary**: HTM
- **neural networks**: GRU, LSTM, TCN, TCNLSTM

Patterns:

- strong **seasonality**.
- week & weekend flows
- night hours, rush hours,

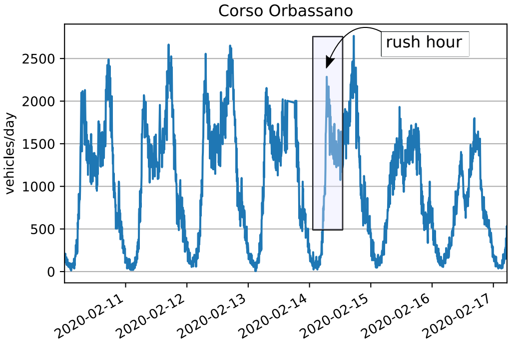

Figure 35: Weekly traffic at Corso Orbassano road.

Predict future traffic $\lambda(t+n)$

- **time-series techniques**: DES, TES
- **proprietary**: HTM
- **neural networks**: GRU, LSTM, TCN, TCNLSTM

Patterns:

- strong **seasonality**.
- week & weekend flows
- night hours, rush hours, schools' out

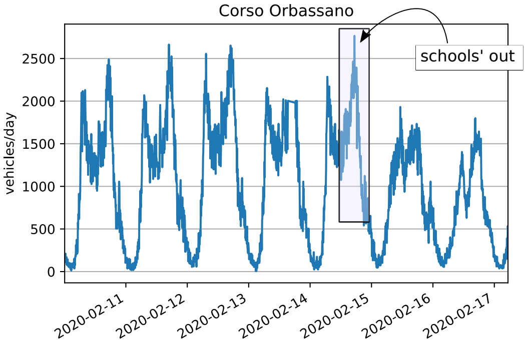

Figure 35: Weekly traffic at Corso Orbassano road.

non-COVID-19 (2020)

- training: 28thFeb - 28thMar
- testing: 29thFeb - 07thMar

COVID-19 (2020)

- training: 06thFeb - 07thMar
- testing: 08thMar - 15thMar

non-COVID-19 (2020)

- training: 28thFeb - 28thMar
- testing: 29thFeb - 07thMar

COVID-19 (2020)

- training: 06thFeb - 07thMar
- testing: 08thMar - 15thMar

Train:

- offline training
- online training

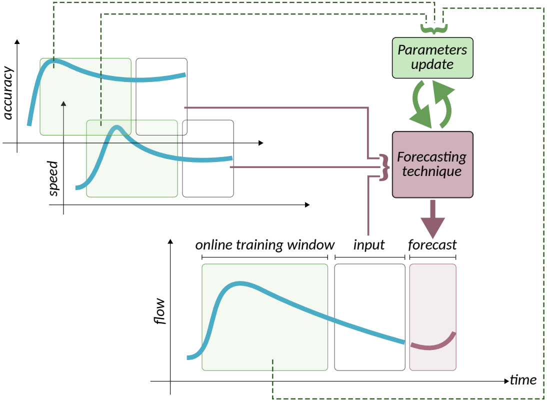

Figure 36: Online training.

Vertical scaling:

1. $\lambda(t+n)$: traffic prediction

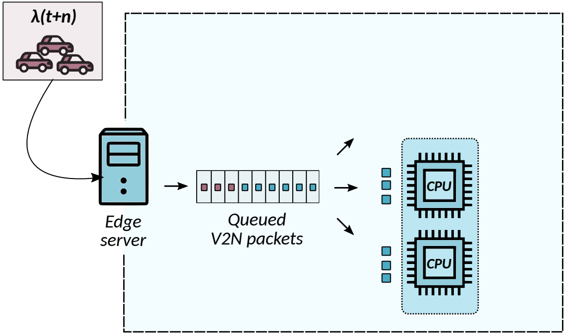

Figure 37: $M/M/c$-based scaling.

Vertical scaling:

1. $\lambda(t+n)$: traffic prediction
2. derive $c(t+n)$ s.t.:

$$\frac{1}{\mu}+\frac{P_Q}{c(t+n)\mu+\lambda(t+n)} \leq D(s) \quad (11)$$

with $D(s)$ the target delay

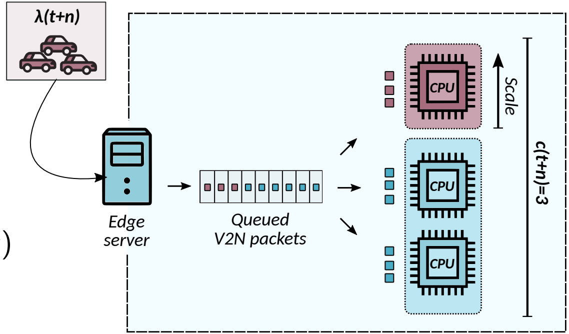

Figure 37: $M/M/c$-based scaling.

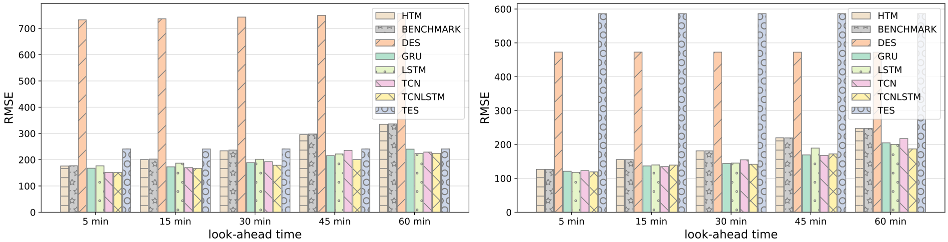

(a) non-COVID-19

(b) COVID-19

Figure 38: Prediction accuracy (offline training).

Most accurate: **Neural Networks**

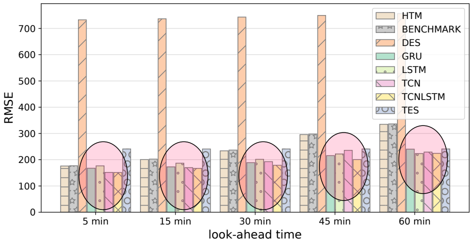

(a) non-COVID-19

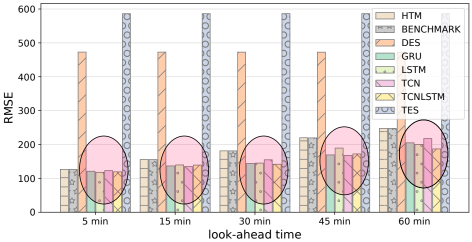

(b) COVID-19

Figure 38: Prediction accuracy (offline training).

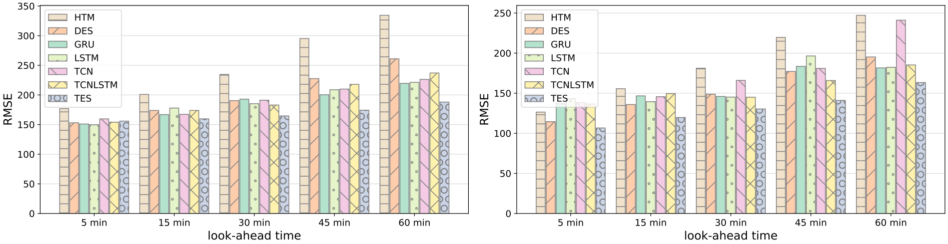

(a) non-COVID-19

(b) COVID-19

Figure 39: Prediction accuracy (online training).

Most accurate: **TES**

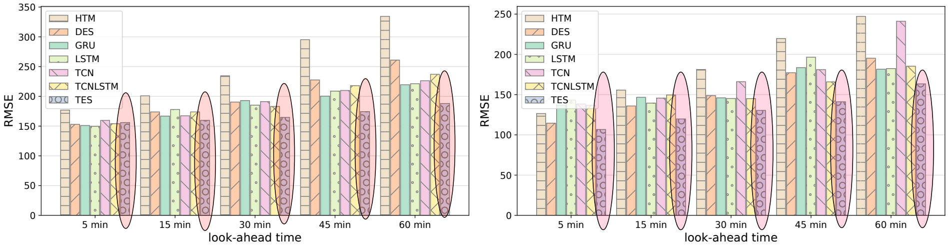

(a) non-COVID-19 (b) COVID-19

Figure 39: Prediction accuracy (online training).

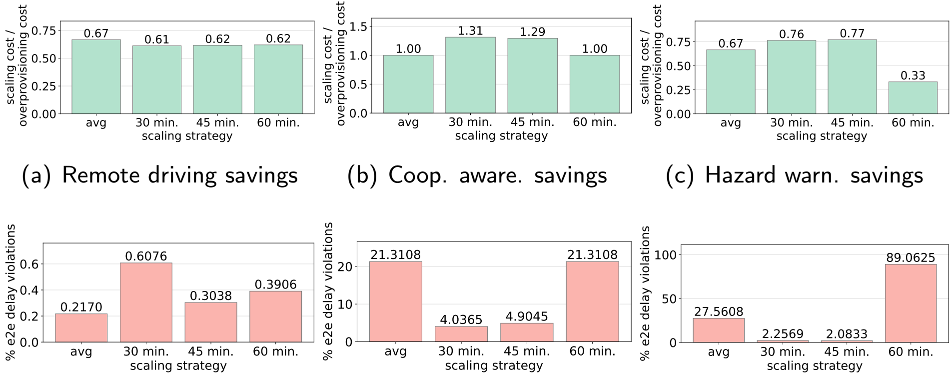

(a) Remote driving savings
(b) Coop. aware. savings
(c) Hazard warn. savings
(d) Remote driving delay violate
(e) Coop. aware. delay violate
(f) Hazard warn. violate

Figure 40: Cost savings and delay violations due to scaling – TES with online training was used.

uc3m

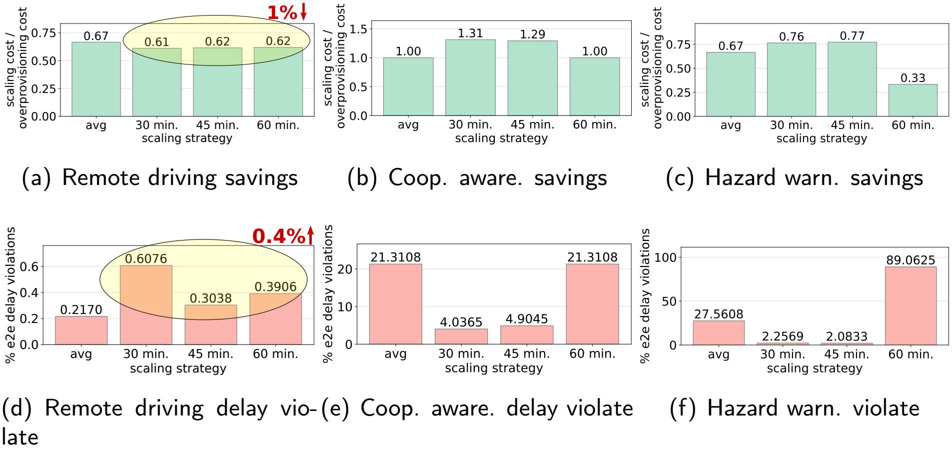

Figure 40: Cost savings and delay violations due to scaling – TES with online training was used.

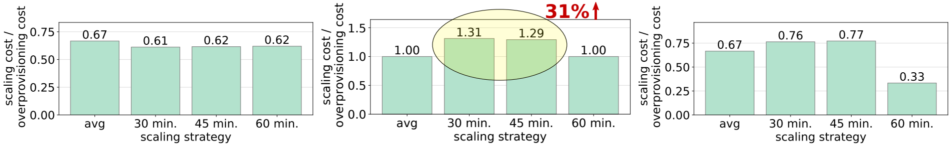

(a) Remote driving savings (b) Coop. aware. savings (c) Hazard warn. savings

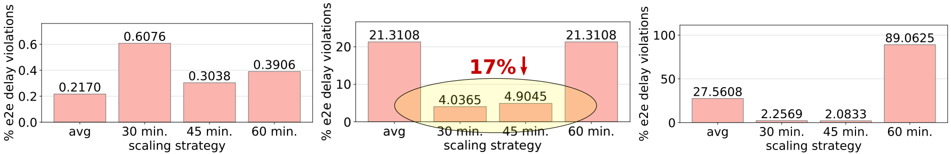

(d) Remote driving delay violate (e) Coop. aware. delay violate (f) Hazard warn. violate

Figure 40: Cost savings and delay violations due to scaling – TES with online training was used.

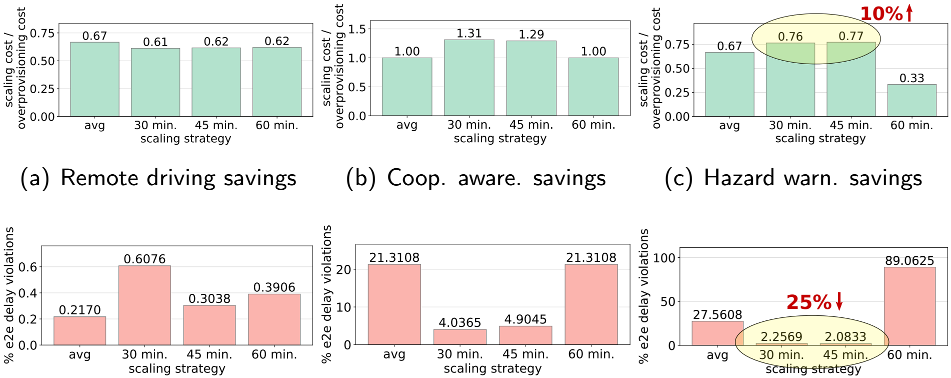

(a) Remote driving savings (b) Coop. aware. savings (c) Hazard warn. savings

(d) Remote driving delay violate (e) Coop. aware. delay violate (f) Hazard warn. violate

Figure 40: Cost savings and delay violations due to scaling – TES with online training was used.

Outline

uc3m

uc3m

Publications:

- D. de Vleeschauwer, J. Baranda, J. Mangues-Bafalluy, C. F. Chiasserini, M. Malinverno, C. Puligheddu, L. Magoula, **Martín-Pérez, J.**, S. Barmpounakis, K. Kondepu, L. Valcarenzhi, X. Li, C. Papagianni, and A. Garcia-Saavedra. "5Growth Data-Driven AI-Based Scaling". In: *2021 EuCNC/6G Summit*. 2021, pp. 383–388. DOI: 10.1109/EuCNC/6GSummit51104.2021.9482476
- **Martín-Pérez, Jorge**, K. Kondepu, D. de Vleeschauwer, V. Reddy, C. Guimarães, A. Sgambelluri, L. Valcarenghi, C. Papagianni, and C. J. Bernardos. "Dimensioning of V2N Services in 5G Networks through Forecast-based Scaling". In: *IEEE Access* (2021). Under review

Open-source (to be released):

- https://github.com/MartinPJorge/5growth-scaling/
- https://github.com/MartinPJorge/5growth-forecasting/

In the **NFV orchestration** process, this thesis contributes to:

In the **NFV orchestration** process, this thesis contributes to:

1. generate **5G graphs** meeting standard requirements

In the **NFV orchestration** process, this thesis contributes to:

1. generate **5G graphs** meeting standard requirements
2. maximize revenue under **federation** and dynamic pricing

In the **NFV orchestration** process, this thesis contributes to:

1. generate **5G graphs** meeting standard requirements
2. maximize revenue under **federation** and dynamic pricing
3. minimize **VNE** cost meeting: latency, reliability, and availability constraints

In the **NFV orchestration** process, this thesis contributes to:

1. generate **5G graphs** meeting standard requirements
2. maximize revenue under **federation** and dynamic pricing
3. minimize **VNE** cost meeting: latency, reliability, and availability constraints
4. reduce the E2E latency violations with the proposed **scaling**

1. **generate federated** scenarios BSs, PoPs & datacenters, all at once

1. **generate federated** scenarios BSs, PoPs & datacenters, all at once
2. **DQN** agent +**LSTM** layer to **predict**

uc3m

1. **generate federated** scenarios BSs, PoPs & datacenters, all at once
2. **DQN** agent +**LSTM** layer to **predict**
3. **OKpi** study on γ/runtime/optimality

1. **generate federated** scenarios BSs, PoPs & datacenters, all at once
2. **DQN** agent +**LSTM** layer to **predict**
3. **OKpi** study on γ/runtime/optimality
4. **V2N scaling** to meet **99.9999%** latency quantile & use **ST-GCN**

uc3m

- **Martín-Pérez, Jorge** and C. J. Bernardos. "Multi-Domain VNF Mapping Algorithms". In: *2018 IEEE International Symposium on Broadband Multimedia Systems and Broadcasting (BMSB)*. 2018, pp. 1–6. DOI: 10.1109/BMSB.2018.8436765
- **Martín-Pérez, Jorge**, L. Cominardi, C. J. Bernardos, and A. Mourad. "5GEN: A tool to generate 5G infrastructure graphs". In: *2019 IEEE Conference on Standards for Communications and Networking (CSCN)*. 2019, pp. 1–4. DOI: 10.1109/CSCN.2019.8931334
- **Martín-Peréz, Jorge**, F. Malandrino, C. F. Chiasserini, and C. J. Bernardos. "OKpi: All-KPI Network Slicing Through Efficient Resource Allocation". In: *IEEE INFOCOM 2020 - IEEE Conference on Computer Communications*. 2020, pp. 804–813. DOI: 10.1109/INFOCOM41043.2020.9155263

- K. Antevski, **J. Martín-Pérez**, A. Garcia-Saavedra, C. J. Bernardos, X. Li, J. Baranda, J. Mangues-Bafalluy, R. Martnez, and L. Vettori. "A Q-learning strategy for federation of 5G services". In: *ICC 2020 - 2020 IEEE International Conference on Communications (ICC)*. 2020, pp. 1–6. DOI: 10.1109/ICC40277.2020.9149082
- D. de Vleeschauwer, J. Baranda, J. Mangues-Bafalluy, C. F. Chiasserini, M. Malinverno, C. Puligheddu, L. Magoula, **Martín-Pérez, J.**, S. Barmpounakis, K. Kondepu, L. Valcarenzhi, X. Li, C. Papagianni, and A. Garcia-Saavedra. "5Growth Data-Driven AI-Based Scaling". In: *2021 EuCNC/6G Summit*. 2021, pp. 383–388. DOI: 10.1109/EuCNC/6GSummit51104.2021.9482476

- **Martín-Pérez, Jorge**, L. Cominardi, C. J. Bernardos, A. de la Oliva, and A. Azcorra. "Modeling Mobile Edge Computing Deployments for Low Latency Multimedia Services". In: *IEEE Transactions on Broadcasting* 65.2 (2019), pp. 464–474. DOI: 10.1109/TBC.2019.2901406
- B. Nemeth, N. Molner, **Martín-Pérez, J.**, C. J. Bernardos, A. de la Oliva, and B. Sonkoly. "Delay and reliability-constrained VNF placement on mobile and volatile 5G infrastructure". In: *IEEE Transactions on Mobile Computing* (2021), pp. 1–1. DOI: 10.1109/TMC.2021.3055426
- **Martín-Pérez, Jorge**, K. Antevski, A. Garcia-Saavedra, X. Li, and C. J. Bernardos. "DQN Dynamic Pricing and Revenue driven Service Federation Strategy". In: *IEEE Transactions on Network and Service Management* (2021), pp. 1–1. DOI: 10.1109/TNSM.2021.3117589

- **Martín-Peréz, Jorge**, F. Malandrino, C. F. Chiasserini, M. Groshev, and C. J. Bernardos. "KPI Guarantees in Network Slicing". In: *IEEE/ACM Transactions on Networking* (2021). Accepted

Thanks for your attention!

uc3m

[1] M. Afshang and H. S. Dhillon. "Poisson Cluster Process Based Analysis of HetNets With Correlated User and Base Station Locations". In: *IEEE Transactions on Wireless Communications* 17.4 (Apr. 2018), pp. 2417–2431. ISSN: 1536-1276. DOI: 10.1109/TWC.2018.2794983.

[2] S. Agarwal, F. Malandrino, C. F. Chiasserini, and S. De. "VNF Placement and Resource Allocation for the Support of Vertical Services in 5G Networks". In: *IEEE/ACM Trans. Netw.* 27.1 (Feb. 2019), pp. 433–446. ISSN: 1063-6692. DOI: 10.1109/TNET.2018.2890631. URL: https://doi.org/10.1109/TNET.2018.2890631.

[3] K. Antevski, **J. Martín-Pérez**, A. Garcia-Saavedra, C. J. Bernardos, X. Li, J. Baranda, J. Mangues-Bafalluy, R. Martnez, and L. Vettori. "A Q-learning strategy for federation of 5G services". In: *ICC 2020 - 2020 IEEE International Conference on Communications (ICC)*. 2020, pp. 1–6. DOI: 10.1109/ICC40277.2020.9149082.

[4] A. Baddeley, C. internazionale matematico estivo, and W. Weil. *Stochastic Geometry: Lectures Given at the C.I.M.E. Summer School Held in Martina Franca, Italy, September 13-18, 2004*. Lecture Notes in Mathematics / C.I.M.E. Foundation Subseries. Springer, 2007. ISBN: 9783540381747.

[5] J. Baranda et al. "Automated deployment and scaling of automotive safety services in 5G-Transformer". In: *2019 IEEE Conference on Network Function Virtualization and Software Defined Networks (NFV-SDN)*. 2019, pp. 1–2. DOI: 10.1109/NFV-SDN47374.2019.9039990.

uc3m

[6] L. Cominardi, L. M. Contreras, C. J. Bernardos, and I. Berberana. "Understanding QoS Applicability in 5G Transport Networks". In: *2018 IEEE International Symposium on Broadband Multimedia Systems and Broadcasting (BMSB)*. June 2018, pp. 1–5. DOI: 10.1109/BMSB.2018.8436847. URL: https://e-archivo.uc3m.es/bitstream/handle/10016/27393/understanding_BMSB_2018_ps.pdf (visited on 01/10/2019).

[7] U. Fattore, M. Liebsch, B. Brik, and A. Ksentini. "AutoMEC: LSTM-Based User Mobility Prediction for Service Management in Distributed MEC Resources". In: *Proceedings of the 23rd International ACM Conference on Modeling, Analysis and Simulation of Wireless and Mobile Systems*. MSWiM '20. Alicante, Spain: Association for Computing Machinery, 2020, pp. 155–159. ISBN: 9781450381178. DOI: 10.1145/3416010.3423246. URL: https://doi.org/10.1145/3416010.3423246.

[8] V. Frascolla et al. "5G-MiEdge: Design, standardization and deployment of 5G phase II technologies: MEC and mmWaves joint development for Tokyo 2020 Olympic games". In: *2017 IEEE Conference on Standards for Communications and Networking (CSCN)*. Sept. 2017, pp. 54–59. DOI: 10.1109/CSCN.2017.8088598.

[9] A. M. Ibrahim, T. ElBatt, and A. El-Keyi. "Coverage probability analysis for wireless networks using repulsive point processes". In: *2013 IEEE 24th Annual International Symposium on Personal, Indoor, and Mobile Radio Communications (PIMRC)*. Sept. 2013, pp. 1002–1007. DOI: 10.1109/PIMRC.2013.6666284.

[10] ITU-T. *Consideration on 5G transport network reference architecture and bandwidth requirements*. Study Group 15 Contribution 0462. International Telecommunication Union - Telecommunication Standardization Sector (ITU-T), Feb. 2018.

[11] G. Li, H. Zhou, B. Feng, and G. Li. "Context-Aware Service Function Chaining and Its Cost-Effective Orchestration in Multi-Domain Networks". In: *IEEE Access* 6 (2018), pp. 34976–34991. DOI: 10.1109/ACCESS.2018.2848266.

[12] F. Malandrino and C. Chiasserini. "Getting the Most Out of Your VNFs: Flexible Assignment of Service Priorities in 5G". In: *2019 IEEE 20th International Symposium on "A World of Wireless, Mobile and Multimedia Networks" (WoWMoM)*. 2019, pp. 1–9. DOI: 10.1109/WoWMoM.2019.8792983.

[13] **Martín-Pérez, Jorge**, K. Antevski, A. Garcia-Saavedra, X. Li, and C. J. Bernardos. "DQN Dynamic Pricing and Revenue driven Service Federation Strategy". In: *IEEE Transactions on Network and Service Management* (2021), pp. 1–1. DOI: 10.1109/TNSM.2021.3117589.

[14] **Martín-Pérez, Jorge** and C. J. Bernardos. "Multi-Domain VNF Mapping Algorithms". In: *2018 IEEE International Symposium on Broadband Multimedia Systems and Broadcasting (BMSB)*. 2018, pp. 1–6. DOI: 10.1109/BMSB.2018.8436765.

[15] **Martín-Pérez, Jorge**, L. Cominardi, C. J. Bernardos, and A. Mourad. "5GEN: A tool to generate 5G infrastructure graphs". In: *2019 IEEE Conference on Standards for Communications and Networking (CSCN)*. 2019, pp. 1–4. DOI: 10.1109/CSCN.2019.8931334.

[16] **Martín-Pérez, Jorge**, L. Cominardi, C. J. Bernardos, A. de la Oliva, and A. Azcorra. "Modeling Mobile Edge Computing Deployments for Low Latency Multimedia Services". In: *IEEE Transactions on Broadcasting* 65.2 (2019), pp. 464–474. DOI: 10.1109/TBC.2019.2901406.

[17] **Martín-Pérez, Jorge**, K. Kondepu, D. de Vleeschauwer, V. Reddy, C. Guimarães, A. Sgambelluri, L. Valcarenghi, C. Papagianni, and C. J. Bernardos. "Dimensioning of V2N Services in 5G Networks through Forecast-based Scaling". In: *IEEE Access* (2021). Under review.

[18] **Martín-Peréz, Jorge**, F. Malandrino, C. F. Chiasserini, and C. J. Bernardos. "OKpi: All-KPI Network Slicing Through Efficient Resource Allocation". In: *IEEE INFOCOM 2020 - IEEE Conference on Computer Communications*. 2020, pp. 804–813. DOI: 10.1109/INFOCOM41043.2020.9155263.

[19] **Martín-Peréz, Jorge**, F. Malandrino, C. F. Chiasserini, M. Groshev, and C. J. Bernardos. "KPI Guarantees in Network Slicing". In: *IEEE/ACM Transactions on Networking* (2021). Accepted.

[20] B. Németh, B. Sonkoly, M. Rost, and S. Schmid. “Efficient service graph embedding: A practical approach”. In: *2016 IEEE Conference on Network Function Virtualization and Software Defined Networks (NFV-SDN)*. 2016, pp. 19–25. DOI: 10.1109/NFV-SDN.2016.7919470.

[21] B. Nemeth, N. Molner, **Martín-Pérez, J.**, C. J. Bernardos, A. de la Oliva, and B. Sonkoly. “Delay and reliability-constrained VNF placement on mobile and volatile 5G infrastructure”. In: *IEEE Transactions on Mobile Computing* (2021), pp. 1–1. DOI: 10.1109/TMC.2021.3055426.

[22] A. Okic, L. Zanzi, V. Sciancalepore, A. Redondi, and X. Costa-Pérez. “π-ROAD: a Learn-as-You-Go Framework for On-Demand Emergency Slices in V2X Scenarios”. In: *IEEE INFOCOM 2021 - IEEE Conference on Computer Communications*. 2021, pp. 1–10. DOI: 10.1109/INFOCOM42981.2021.9488677.

[23] P. T. A. Quang, A. Bradai, K. D. Singh, G. Picard, and R. Riggio. "Single and Multi-Domain Adaptive Allocation Algorithms for VNF Forwarding Graph Embedding". In: *IEEE Transactions on Network and Service Management* 16.1 (2019), pp. 98–112. DOI: 10.1109/TNSM.2018.2876623.

[24] I. Sarrigiannis, L. M. Contreras, K. Ramantas, A. Antonopoulos, and C. Verikoukis. "Fog-Enabled Scalable C-V2X Architecture for Distributed 5G and Beyond Applications". In: *IEEE Network* 34.5 (2020), pp. 120–126. DOI: 10.1109/MNET.111.2000476.

[25] V. Sciancalepore, F. Z. Yousaf, and X. Costa-Perez. "z-TORCH: An Automated NFV Orchestration and Monitoring Solution". In: *IEEE Transactions on Network and Service Management* 15.4 (2018), pp. 1292–1306. DOI: 10.1109/TNSM.2018.2867827.

[26] A. Solano and L. M. Contreras. "Information Exchange to Support Multi-Domain Slice Service Provision for 5G/NFV". In: *2020 IFIP Networking Conference (Networking)*. 2020, pp. 773–778.

[27] V. Suryaprakash, J. Møller, and G. Fettweis. "On the Modeling and Analysis of Heterogeneous Radio Access Networks Using a Poisson Cluster Process". In: *IEEE Transactions on Wireless Communications* 14.2 (Feb. 2015), pp. 1035–1047. ISSN: 1536-1276. DOI: 10.1109/TWC.2014.2363454.

[28] V. Suryaprakash, P. Rost, and G. Fettweis. "Are Heterogeneous Cloud-Based Radio Access Networks Cost Effective?" In: *IEEE Journal on Selected Areas in Communications* 33.10 (Oct. 2015), pp. 2239–2251. ISSN: 0733-8716. DOI: 10.1109/JSAC.2015.2435275.

[29] M. Syamkumar, P. Barford, and R. Durairajan. “Deployment Characteristics of "The Edge" in Mobile Edge Computing”. In: *Proceedings of the 2018 Workshop on Mobile Edge Communications*. MECOMM'18. Budapest, Hungary: ACM, 2018, pp. 43–49. ISBN: 978-1-4503-5906-1. DOI: 10.1145/3229556.3229557. URL: http://doi.acm.org/10.1145/3229556.3229557.

[30] D. de Vleeschauwer et al. “5Growth Data-Driven AI-Based Scaling”. In: *2021 EuCNC/6G Summit*. 2021, pp. 383–388. DOI: 10.1109/EuCNC/6GSummit51104.2021.9482476.

[31] H. Xu and B. Li. “Dynamic cloud pricing for revenue maximization”. In: *IEEE Transactions on Cloud Computing* 1.2 (2013), pp. 158–171.

[32] Q. Zhang, F. Liu, and C. Zeng. “Adaptive Interference-Aware VNF Placement for Service-Customized 5G Network Slices”. In: *IEEE INFOCOM 2019 - IEEE Conference on Computer Communications*. 2019, pp. 2449–2457. DOI: 10.1109/INFOCOM.2019.8737660.

[33] Q. Zhang, X. Wang, I. Kim, P. Palacharla, and T. Ikeuchi. “Service function chaining in multi-domain networks”. In: *2016 Optical Fiber Communications Conference and Exhibition (OFC)*. 2016, pp. 1–3.

Lemma

Given an inhomogeneous marked PPP X with intensity function λ, the thinning function l_2, and marks $m \sim \frac{1}{\lambda(x)}$, the resulting thinned point process, called inhomogeneous Matérn II PP, has the following average number of points at C:

$$\mathbb{E}\left[N(C)\right] := \int_C e^{-\int_{B(x,r)} \mathbb{1}(\lambda(u) > \lambda(x))\lambda(u)du} \lambda(x)\ dx \tag{12}$$

where r is the thinning radius of l_2.

with

$$l_2(x, m, X, M_X) := \begin{cases} 1 & \text{if } m = \min_{m' \in M_X} \left\{(x', m') : x' \in B(x, r)\right\} \\ 0 & \text{otherwise} \end{cases} \tag{13}$$

The RTT considered is computed as

$$RTT := 2l\left(\|x - m\|_1\right) + 2p(M) + UL + DL \tag{14}$$

We find m_M, the maximum distance from MEC PoP m to the BS at position x, as:

$$\|x - m\|_1 \leq l^{-1}\left(\frac{RTT - 2p(M) - t_r}{2}\right) = m_M \tag{15}$$

with $\|\cdot\|_1$ denoting the Manhattan distance.

User pays $p^{(t)}$ for the service σ

$$p^{(t)}(\sigma) = (1+P)l^{(t)}(\sigma) \tag{16}$$

with P the profit margin, and $l^{(t)}$ the local deployment cost (based on uncertain phenomena).

User pays $p^{(t)}$ for the service σ

$$p^{(t)}(\sigma) = (1+P)I^{(t)}(\sigma) \tag{16}$$

with P the profit margin, and $I^{(t)}$ the local deployment cost (based on uncertain phenomena).

Given the federation fee $f(\sigma)$ the **reward** is:

$$r^{(t)}(X_t) := \sum_{\substack{\sigma:\ x(\sigma)=0 \\ a(\sigma)\leq t\leq d(\sigma)}} p^{a(\sigma)}(\sigma) + \sum_{\substack{\sigma:\ x(\sigma)=1 \\ a(\sigma)\leq t\leq d(\sigma)}} \left[p^{a(\sigma)}(\sigma) - f^{(t)}(\sigma)\right] \tag{17}$$

where $X_t := \{x(\sigma)\}_{\sigma:a(\sigma)\leq t}$.

uc3m

$$f(p^{(t)}(\sigma)) := \begin{cases} k\left(1-\left(\frac{p^{(t)}(\sigma)}{K\cdot M}\right)^{a}\right)^{b}, & p^{(t)}(\sigma) \leq K\cdot M \\ 0, & p^{(t)}(\sigma) > K\cdot M \end{cases} \tag{18}$$

where $M = \max_{\sigma,t}\{l^{(t)}(\sigma)\}$ is the maximum local deployment cost over time across all services σ (e.g., *t3a.small*), and K is a normalization constant to control the decay of the arrival rate.

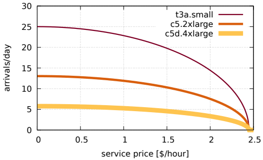

Figure 41: Impact of prices on arriving users.

Increase of P leads to:

- less user arrivals
- larger reward

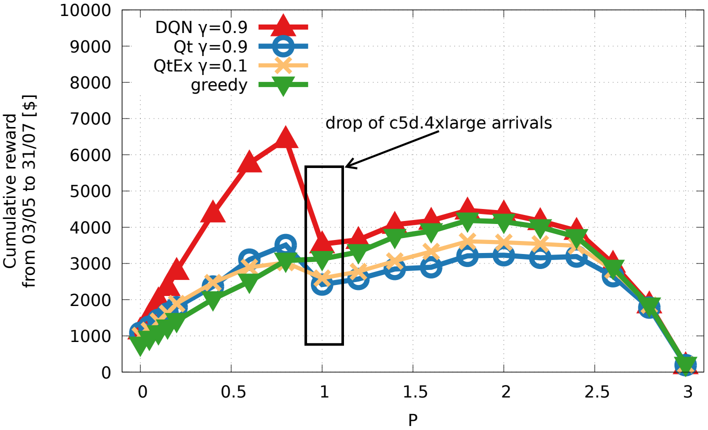

Figure 42: Impact of the marginal benefit P in the commutative reward achieved by each solution.